

NISTIR 89-4035

NEW NIST PUBLICATION
June 12, 1989



Considerations of Stack Effect in Building Fires

John H. Klote

U.S. DEPARTMENT OF COMMERCE
National Institute of Standards and Technology
National Engineering Laboratory
Center for Fire Research
Gaithersburg, MD 20899

January 1989

Issued May 1989

Sponsored by:
U.S. Fire Administration
Emmitsburg, MD 21727

NISTIR 89-4035

Considerations of Stack Effect in Building Fires

John H. Klote

U.S. DEPARTMENT OF COMMERCE
National Institute of Standards and Technology
National Engineering Laboratory
Center for Fire Research
Gaithersburg, MD 20899

January 1989

Issued May 1989



National Bureau of Standards became the National Institute of Standards and Technology on August 23, 1988, when the Omnibus Trade and Competitiveness Act was signed. NIST retains all NBS functions. Its new programs will encourage improved use of technology by U.S. industry.

Sponsored by:
U.S. Fire Administration
Emmitsburg, MD 21727

U.S. DEPARTMENT OF COMMERCE
Robert Mosbacher, Secretary
NATIONAL INSTITUTE OF STANDARDS
AND TECHNOLOGY
Raymond G. Kammer, Acting Director

TABLE OF CONTENTS

LIST OF FIGURES	v
LIST OF TABLES	viii
Abstract	1
1. INTRODUCTION	2
2. DRIVING FORCES OF SMOKE MOVEMENT	2
2.1 Stack Effect	3
2.2 Buoyancy of Combustion Gases	11
2.3 Expansion of Combustion Gases	12
2.4 Wind Effect	13
2.5 Ventilation Systems	16
2.6 Elevator Piston Effect	17
3. LOCATION OF NEUTRAL PLANE	22
3.1 Shaft with a Continuous Opening	22
3.2 Shaft With Two Vents	24
3.3 Vented Shaft	26
4. FRICTION LOSS IN SHAFTS	28
5. STEADY SMOKE CONCENTRATIONS	30
6. NETWORK MODELS	31
6.1 Network Model Concept	32
6.2 Mass Flow Rates	32
6.3 Unsteady Smoke Concentrations	34
6.4 Unsteady Temperatures	36
7. ZONE MODELS	36
7.1 Compartment Fire Phenomena	37
7.2 Application to High Rise Buildings	41
8. STEADY FLOW NETWORK CALCULATIONS	47
8.1 Building with Doors Closed and No Vents (Case 1)	50
8.2 Top Vented Elevator Shaft (Case 2)	57
8.3 Top Vented Stair Shaft (Case 3)	58
8.4 Top Vents on Stair and Elevator Shafts (Case 4)	59
8.5 Top and Bottom Vented Stair Shaft (Case 5)	59
8.6 Bottom Vented Stair Shaft (Case 6)	60
8.7 Effect of Elevated Temperatures (Cases 4A and 6A)	61
8.8 Fire Above the Neutral Planes	62

TABLE OF CONTENTS Continued

9.	FUTURE EFFORT	67
	9.1 Full Scale Experiments	68
	9.2 Scale Model Experiments	69
10.	CONCLUSIONS	69
11.	ACKNOWLEDGMENTS	71
12.	NOMENCLATURE	71
13.	REFERENCES	72

LIST OF FIGURES

Figure 1.	Air movement due to normal and reverse stack effect	4
Figure 2.	Pressures and pressure differences occurring during normal stack effect	5
Figure 3.	Comparison of measured and calculated pressure differences across the outside wall of the Canadian Fire Research Tower for different outside temperatures	9
Figure 4.	Comparison of measured and calculated pressure differences across a shaft enclosure of the Canadian Fire Research Tower for different building leakages	10
Figure 5.	Pressures occurring during a fully involved compartment fire .	11
Figure 6.	Wind velocity profiles for flat and very rough terrain	16
Figure 7.	Airflow due to downward movement of elevator car	18
Figure 8.	Pressure difference, ΔP_{1i} , across elevator lobby of a Toronto hotel due to piston effect	20
Figure 9.	Calculated upper limit of the pressure difference, $(\Delta P_{1i})_u$, from the elevator lobby to the building due to piston effect	21
Figure 10.	Normal stack effect between a single shaft connected to the outside by a continuous opening	22
Figure 11.	Stack effect for a shaft with two openings	24
Figure 13.	Stratified smoke flow as simulated by zone fire models	37
Figure 14.	Smoke flow at 0.5 minutes after ignition in a ten story building calculated by a zone model	42
Figure 15.	Smoke flow at 1.0 minutes after ignition in a ten story building calculated by a zone model	43
Figure 16.	Smoke flow at 3.0 minutes after ignition in a ten story building calculated by a zone model	44
Figure 17.	Smoke flow at 4.5 minutes after ignition in a ten story building calculated by a zone model	45

LIST OF FIGURES Contents

Figure 18.	Floor plan of building used for example analyses	48
Figure 19.	Calculated smoke concentrations due to a fourth floor fire in a 20 story building without any vents or open doors (Case 1)	51
Figure 20.	Calculated smoke concentrations due to a fourth floor fire in a 20 story building with a top vented elevator shaft (Case 2)	52
Figure 21.	Calculated smoke concentrations due to a fourth floor fire in a 20 story building with a top vented stairwell (Case 3)	53
Figure 22.	Calculated smoke concentrations due to a fourth floor fire in a 20 story building with top vents in elevator and stair shafts (Case 4)	54
Figure 23.	Calculated smoke concentrations due to a fourth floor fire in a 20 story with top vents in elevator and stair shafts and an open stair door (Case 5)	55
Figure 24.	Calculated smoke concentrations due to a fourth floor fire in a 20 story building with top vents in elevator and stairwell shafts and with an open stairwell door (Case 6)	56
Figure 25.	Pressures for a building with a top vented shaft	58
Figure 26.	Pressures for a building with a shaft vented at the top and bottom	60
Figure 27.	Pressures for a building with a bottom vented shaft	61
Figure 28.	Calculated smoke concentrations due to a fourth floor fire in a 20 story building with top vents in elevator and stairwell shafts and with elevated shaft temperatures (Case 4A)	63
Figure 29.	Calculated smoke concentrations due to a fourth floor fire in a 20 story building with a top vented elevator, with an open stairwell door, and with elevated shaft temperatures (Case 6A)	64

LIST OF FIGURES Contents

Figure 30. Calculated smoke concentrations due to a fifteenth floor fire in a 20 story building with a top vented elevator shaft (Modification of case 2) 65

Figure 31. Calculated smoke concentrations due to a fifteenth floor fire in a 20 story building with a top vented stairwell (Modification of case 3) 66

LIST OF TABLES

Table 1.	Comparison of pressure differences due to various driving forces	7
Table 2.	Average pressure coefficients for walls of rectangular buildings	14
Table 3.	Dimensions used for Tanaka's (1983) zone model simulation of smoke movement in a ten story building	41
Table 4.	Flow areas and other data about building for example analyses	47
Table 5.	List of vent and door conditions for example analyses	50
Table 6.	Calculated flow rates (lb/min) in a building without any vents or open doors (Case 1)	76
Table 7.	Calculated flow rates (lb/min) in a building with a top vented elevator shaft (Case 2)	77
Table 8.	Calculated flow rates (lb/min) in a building with a top vented stairwell (Case 3)	78
Table 9.	Calculated flow rates (lb/min) in a building with a top vented elevator shaft and a top vented stairwell (Case 4)	79
Table 10.	Calculated flow rates (lb/min) in a building with a top vented elevator shaft and a stairwell with a top vent and an open exterior door (Case 5)	80
Table 11.	Calculated flow rates (lb/min) in a building with a top vented elevator shaft and a stairwell with an open exterior door (Case 6)	81
Table 12.	Calculated flow rates (lb/min) in a building with top vented elevator shaft and stairwell and with elevated shaft and fire floor temperatures (Case 4A)	82
Table 13.	Calculated flow rates (lb/min) in a building with a top vented elevator shaft, with a stairwell with an open exterior door, and with elevated shaft and fire floor temperatures (Case 6A)	83

CONSIDERATIONS OF STACK EFFECT IN BUILDING FIRES

John H. Klote

Abstract

The following driving forces of smoke movement in buildings are discussed: stack effect, buoyancy of combustion gases, expansion of combustion gases, wind effect, and elevator piston effect. Based on an analysis of elevator piston effect, it is concluded that the likelihood of smoke being pulled into an elevator shaft due to elevator car motion is greater for single car shafts than for multiple car shafts. Methods of evaluating the location of the neutral plane are presented. It is shown that the neutral plane between a vented shaft and the outside is located between the neutral plane height for an unvented shaft [equation (23)] and the vent elevation. Calculations are presented that show that pressure losses due to friction are generally negligible for unvented shafts with all doors closed. The capabilities and limitations of network models and zone models are discussed. The network method was applied to several cases of open and closed doors and shaft vents likely to occur during firefighting. For the cases evaluated, shaft venting did not result in any significant reduction in smoke concentrations on the floors of the building. One of the cases showed that for low outside temperatures, bottom venting of a shaft can result in shaft pressurization. Other cases demonstrated that elevated temperatures of combustion gases can result in downward smoke flow from one floor to another. Much of the information in this paper is applicable to the migration of other airborne matter such as hazardous gases and bacteriological or radioactive matter.

Key words: elevators, smoke vents, smoke transport, stack effect, stairwells, wind effects.

1. INTRODUCTION

In building fires, smoke often migrates to locations remote from the fire space. Stairwells and elevator shafts frequently become smoke-logged, thereby blocking evacuation and inhibiting fire fighting. In this paper several of the driving forces of smoke movement are discussed. The steady flow analysis of stack effect and some considerations of unsteady flow are addressed. The steady flow methods are applied to situations of open doors and shaft vents likely to occur during firefighting. A number of generalizations which could be of use to fire fighters are presented. The information in this paper also is applicable to the migration of other airborne matter such as hazardous gases, bacteriological matter or radioactive matter in laboratories, hospitals, or industrial facilities. However, the discussion in this paper is primarily aimed at smoke movement.

This paper does not address the pressurization approach to the smoke movement problem. This approach is referred to as smoke control and is addressed in the National Fire Protection Association (NFPA) recommended practice 92A (1988) and the American Society of Heating, Refrigerating and Air ASHRAE Smoke Control Manual (Klote and Fothergill 1983).

In this paper the term smoke is used in accordance with the NFPA 92A (NFPA 1988) definition which states that smoke consists of the airborne solid and liquid particulates and gases evolved when a material undergoes pyrolysis or combustion, together with the quantity of air that is entrained or otherwise mixed into the mass.

2. DRIVING FORCES OF SMOKE MOVEMENT

The driving forces of smoke movement include naturally occurring stack effect, buoyancy of combustion gases, expansion of combustion gases, the wind effect, fan powered ventilation systems, and elevator piston effect. This report discusses these driving forces, and in particular addresses smoke

movement due to the stack effect process, either naturally occurring or that of combustion gases. Stack effect is discussed here as acting alone in order to facilitate discussion and analysis. While other driving forces may act in conjunction with stack effect, there are cases where stack effect is the dominate driving force. Consideration of stack effect acting in the absence of other driving forces can lead to an understanding of smoke transport for these cases.

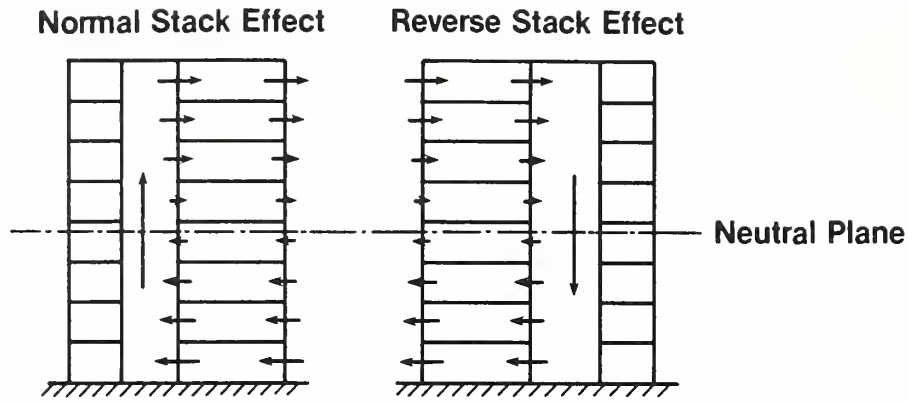
2.1 Stack Effect

Frequently when it is cold outside, there is an upward movement of air within building shafts, such as stairwells, elevator shafts, dumbwaiters shafts, mechanical shafts, and mail chutes. Air in the building has a buoyant force because it is warmer and therefore less dense than outside air. The buoyant force causes air to rise within building shafts. This phenomenon is called by various names such as stack effect, stack action, and chimney effect. These names come from the comparison with the upward flow of gases in a smoke stack or chimney. However, a downward flow of air can occur in air conditioned buildings when it is hot outside. For this paper, the upward flow will be called normal stack effect, and the downward flow will be called reverse stack effect as illustrated in figure 1.

Most building shafts have relatively large cross sectional areas, and for most flows typical of those induced by stack effect the friction losses are negligible in comparison with pressure differences due to buoyancy. Accordingly, this analysis is for negligible shaft friction, but shaft friction is specifically addressed later. Pressure, P_s , within a shaft is due to fluid static forces and can be expressed as

$$dP_s = - \rho_s g dz \quad (1)$$

where g is the acceleration of gravity, z is elevation, and ρ_s is gas density inside the shaft. For the elevations relevant to buildings, the acceleration of gravity can be considered constant. For constant density, equation (1) can be integrated from $z = 0$ to $z = h$ to yield



Note: Arrows Indicate Direction of Air Movement

Figure 1. Air movement due to normal and reverse stack effect

$$P_s = P_a - \rho_s g h \quad (2)$$

where P_a is the pressure at $h = 0$. To simplify the analysis, the vertical coordinate system is selected such that $P_s = P_o$ at $h = 0$. In the absence of wind effects, the outside pressure, P_o , is

$$P_o = P_a - \rho_o g h \quad (3)$$

where ρ_o is the density outside the shaft. Pressures inside the shaft and outside the building are graphically illustrated in figure 2 for normal stack effect. This figure also shows the pressure of the building spaces, and methods of calculating this are presented later in this section. The pressure difference, ΔP_{s_o} , from the inside to the outside is expressed as

$$\Delta P_{s_o} = P_s - P_o = (\rho_o - \rho_s) g h \quad (4)$$

Because variations in pressure within a building are very small compared to atmospheric pressure, atmospheric pressure, P_{atm} , can be used in calculating gas density, ρ , from the ideal gas equation.

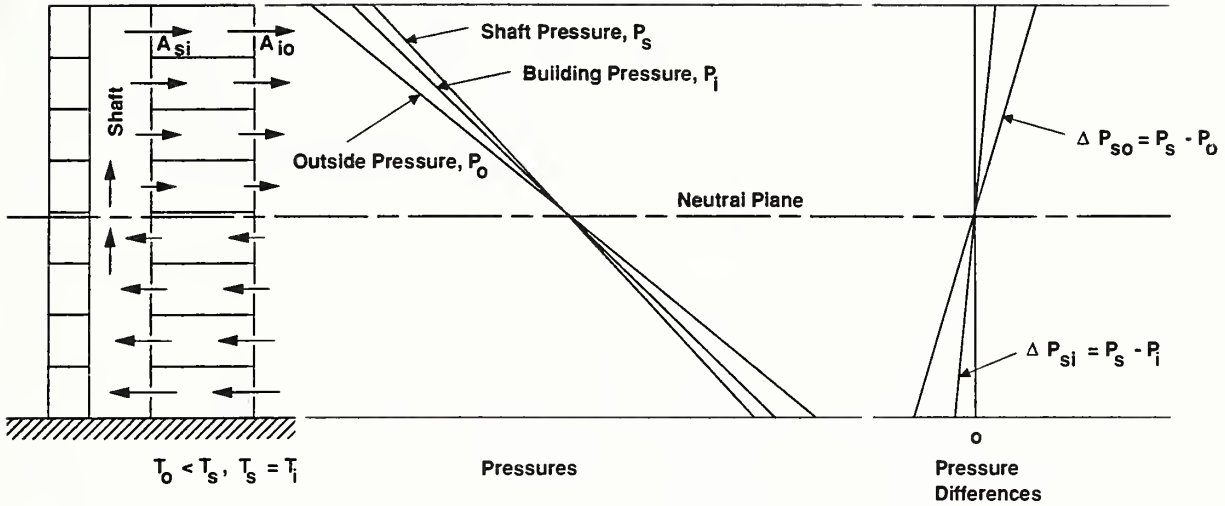


Figure 2. Pressures and pressure differences occurring during normal stack effect

$$\rho = \frac{P_{atm}}{R T} \quad (5)$$

where R is the gas constant of a air, and T is the absolute temperature of air. Substituting equation (5) into equation (4), and rearranging results in the following equation.

$$\Delta P_{s_o} = \frac{g P_{atm}}{R} \left(\frac{1}{T_o} - \frac{1}{T_s} \right) h \quad (6)$$

where T_o is the absolute temperature of outside air, and T_s is the absolute temperature of air inside the shaft. Equation (6) was developed for a shaft connected to the outside. The neutral plane is a horizontal plane located at $h = 0$ where the pressure inside equals that outside. If the location of the neutral plane is known, this equation can be used to determine the pressure

difference from the inside to the outside regardless of variations in building leakage or the presence of other shafts.

For example, if the neutral plane is located at the mid height of a 600 ft (185 m) tall building¹ with inside and outside temperatures of 70 °F (21 C) and 0 °F (-18 C), pressure difference due to stack effect is .66 in H₂O (164 Pa) at the top of the shaft. Methods of determining the location of the neutral plane are discussed later. Table 1 is a comparison of pressure differences due to various driving forces.

The concept of the effective flow area can be used to evaluate the pressure, P_i , on the floor. The effective area of a system of flow areas is the area that results in the same flow as the system when it is subjected to the same pressure difference over the total system of flow paths. Readers are referred to Klote and Fothergill (1983) for a detailed discussion of effective flow areas. In general, for flow areas, A_i , in series where i is from 1 to n , the effective area, A_e , is

$$A_e = \left(\sum_j^n A_j^{-2} \right)^{-\frac{1}{2}} \quad (7)$$

This relation assumes that the flows can only occur in one direction at any flow path and that the air temperatures in the paths are the same. For the system of flow paths illustrated in figure 2, the effective flow area per floor is

$$A_e = \left(\frac{1}{A_{s_i}^2} + \frac{1}{A_{i_o}^2} \right)^{-\frac{1}{2}} \quad (8)$$

where A_{s_i} is the per floor area between the shaft and the building, and A_{i_o} is the per floor area between the building and the outside. The mass flow rate,

¹This means that $h = 300$ ft (92.5 m) at the top of the building.

Table 1. Comparison of pressure differences due to various driving forces

Driving Force	Location of ΔP	Conditions	ΔP in H_2O (Pa)
Stack Effect [Equation (6)]:	Shaft to Outside	Note: For all stack effect examples, $T_s = 70^\circ F$ (21 $^\circ C$), and $T_o = 0^\circ F$ (-18 $^\circ C$). $h = 30$ ft (9.25 m) $h = 300$ ft (92.5 m) $h = 1000$ ft (305 m)	0.07 (17) 0.66 (160) 2.2 (550)
[Equation (9)]:	Shaft to Building	For $A_{si}/A_{io} = 1.7$: $h = 30$ ft (9.25 m) $h = 300$ ft (92.5 m) $h = 1000$ ft (305 m)	0.02 (5) 0.17 (42) 0.57 (140)
Buoyancy of Combustion Gases [Equation (11)]:	Fire Room to Adjacent Room at Ceiling	For $A_{si}/A_{io} = 7$: $h = 30$ ft (9.25 m) $h = 300$ ft (92.5 m) $h = 1000$ ft (305 m)	0.001 (0.2) 0.01 (2) 0.04 (10)
Wind Effect [Equation (14)]:	Across the Building (Windward Wall to Leeward Wall)	$T_f = 1600^\circ F$ (870 $^\circ C$), $T_o = 70^\circ F$ (21 $^\circ C$), and $h = 5.6$ ft (1.71 m) $T_f = 1290^\circ F$ (700 $^\circ C$), $T_o = 70^\circ F$ (21 $^\circ C$), and $h = 35$ ft (10.7 m) Note: For all the wind effect examples, $\rho_o = 0.075$ lb/ft ³ (1.2 kg/m ³), $C_{w1} = 0.8$, and $C_{w2} = -0.8$. $U = 5$ mph (2.24 m/s) $U = 10$ mph (4.47 m/s) $U = 25$ mph (11.2 m/s) $U = 50$ mph (22.4 m/s)	0.02 (5) 0.08 (20) 0.48 (120) 1.9 (470)
Ventilation Systems	Across Barrier of Smoke of Control System	Note: Values based on experience	0.05 to 0.30 (12 to 75)
Elevator Piston Effect [Equations (17) and (19)]:	From Elevator Lobby to Building	Note: For all the examples of the upper limit of pressure difference due elevator car motion, $\rho = 0.75$ lb/ft ³ (1.20 kg/m ³), $A_{ls} = 1.60$ ft ² (0.149 m ²), $A_{il} = 0.42$ ft ² (0.039 m ²), $A_{oi} = 0.54$ ft ² (0.0502 m ²). For a single car shaft with $C_c = 0.83$, $A_s = 60.4$ ft ² (5.61 m ²), $A_f = 19.4$ ft ² (1.80 m ²): $U = 400$ ft/min (2.03 m/s) $U = 700$ ft/min (3.56 m/s) For a double car shaft with $C_c = 0.94$, $A_s = 120.8$ ft ² (11.22 m ²), $A_f = 79.8$ ft ² (7.41 m ²): $U = 400$ ft/min (2.03 m/s) $U = 700$ ft/min (3.56 m/s)	0.08 (20) 0.26 (65) 0.02 (5) 0.05 (12)

m, at a floor can be expressed as $C A_e (2 \rho \Delta P_{s_o})^{1/2}$, where C is a dimensionless flow coefficient which is generally in the range of 0.6 to 0.7. For paths in series the pressure difference across one path equals the pressure difference across the system times the square of the ratio of the effective area of the system to the flow area of the path in question. Thus the pressure difference from the shaft to the building space is $\Delta P_{s_i} = \Delta P_{s_o} (A_e/A_{s_i})^2$. By substituting equation (8) into this relation and rearranging, the effective area is eliminated.

$$\Delta P_{s_i} = \frac{\Delta P_{s_o}}{1 + (A_{s_i}/A_{i_o})^2} \quad (9)$$

In general, the ratio A_{s_i}/A_{i_o} varies from about 1.7 to 7. The pressure differences from a shaft to the building space are much less than those from the shaft to the outside, as can be seen from the examples listed in table 1. In the event that many windows on the fire floor break due to the fire, the value of A_{i_o} becomes very large on the fire floor. When this happens, the ratio A_{s_i}/A_{i_o} becomes very small, and ΔP_{s_i} approaches ΔP_{s_o} . Thus when a large number of windows break on the fire floor, the pressure from the shaft to the building is almost the same as that from the shaft to the outside.

The development of equation (9) considered the pressure difference uniform with height at each floor which introduces an error the maximum value of which can be calculated by equation (6) for a value of h equal to the distance between floors. In the examples of table 1, if the floors were 10 ft (3.1 m) apart, the maximum error of equation (9) is about .01 in H_2O (2.5 Pa). In general, this error is not significant. Equation (9) can be rewritten for the pressure, P_i , at the building space.

$$P_i = P_s - \frac{\Delta P_{s_o}}{1 + (A_{s_i}/A_{i_o})^2} \quad (10)$$

The series flow approach to determining building pressures described above can be used for buildings with multiple shafts, if all the shafts are at

the same pressures and if all the shafts have the same starting and ending elevations. Pressure measurements on several buildings (Tamura and Wilson 1966, 1967a, 1967b) verify the stack effect theory presented above for conditions encountered in the field. Additionally, Tamura and Klote (1988) have conducted full scale stack effect experiments at the Canadian ten story Fire Research Tower near Ottawa which verified the stack effect theory for a range of temperatures and of leakage conditions they considered representative of most buildings. Figure 3 shows comparisons of measured and calculated

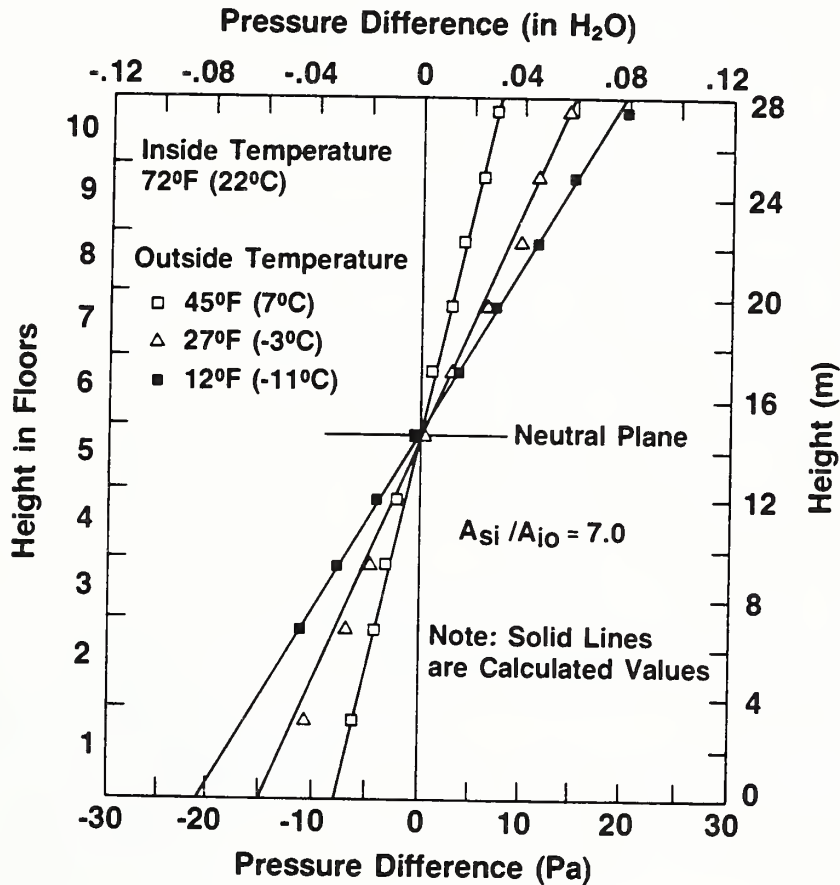


Figure 3. Comparison of measured and calculated pressure differences across the outside wall of the Canadian Fire Research Tower for different outside temperatures [Adapted from Tamura and Klote (1988)]

pressure differences due to stack effect for outside temperatures of 12 °F (-11 °C), 27 °F (-3 °C) and 45 °F (7 °C). Figure 4 shows comparisons of measured and calculated pressure differences for ratios A_{s_i}/A_{i_o} of 1.7, 2.4 and 7. Further, this stack effect theory provides a useful approximation for buildings for which all of the shafts do not have the same starting and ending elevations.

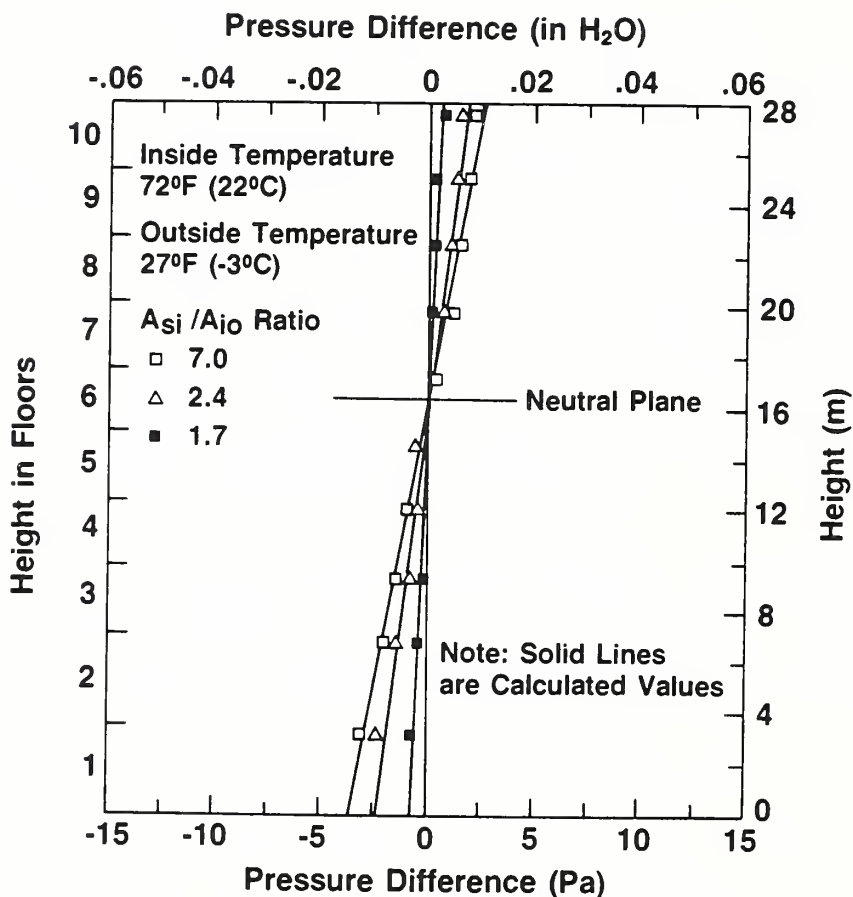


Figure 4. Comparison of measured and calculated pressure differences across a shaft enclosure of the Canadian Fire Research Tower for different building leakages [Adapted from Tamura and Klote (1988)]

2.2 Buoyancy of Combustion Gases

High temperature smoke from a fire has a buoyancy force due to its reduced density. The pressures occurring during a fully involved compartment fire are illustrated in figure 5, and these pressures can be analyzed in the same manner as pressures due to stack effect. In the same manner as equation (6) was developed for stack effect, the following equation for the pressure difference, ΔP_{f_o} , from the fire compartment to its surroundings can be developed

$$\Delta P_{f_o} = \frac{g P_{atm}}{R} \left(\frac{1}{T_o} - \frac{1}{T_f} \right) h \quad (11)$$

where T_o is the temperature of the gases surrounding the fire compartment, T_f is the gas temperature within the fire compartment, and h is the height above the neutral plane between the fire compartment and its surroundings. This equation is for a constant fire-compartment temperature. For a fire-compartment temperature of 1470 °F (800 °C), the pressure difference 6 ft (1.83 m) above the neutral plane is about 0.06 in H_2O (15 Pa). Fang (1980) has studied pressure differences caused by the stack effect of a room fire

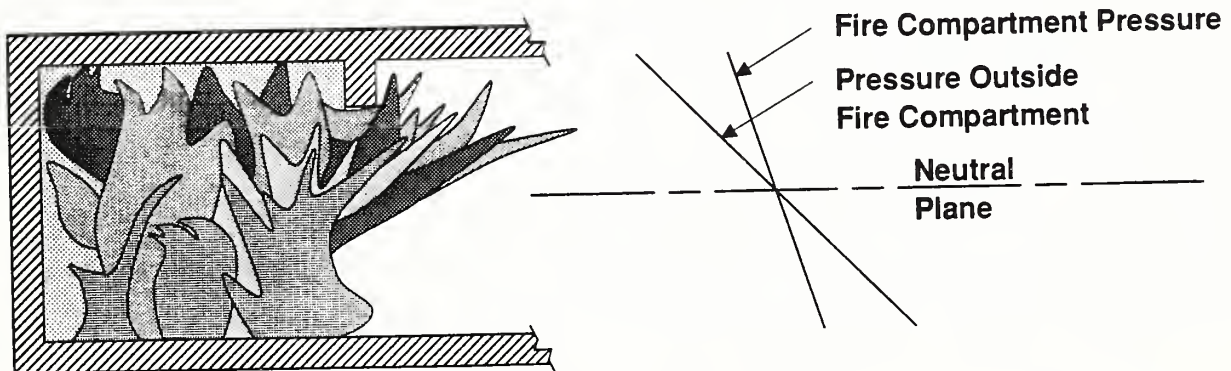


Figure 5. Pressures occurring during a fully involved compartment fire

during a series of full scale fire tests. During these tests, the maximum pressure difference reached was 0.064 in H₂O (16 Pa) across the burn room wall at the ceiling.

Observation of table 1 can provide insight on conditions for which buoyancy as opposed to stack effect is likely to be the dominate driving force. Without broken windows, the buoyancy will dominate for large values of A_{s_i}/A_{i_o} at almost any location from the neutral plane. For low values of A_{s_i}/A_{i_o} at locations far from the neutral plane, stack effect can dominate even when windows are unbroken. When windows are broken, stack effect is even more likely to dominate. Of course, stack effect can only be the dominate driving force during times of significant inside-to-outside temperature difference.

Much larger pressure differences are possible for tall fire compartments where the distance, h, from the neutral plane can be larger. If the fire compartment temperature is 1290 °F (700 °C), the pressure difference 35 ft (10.7 m) above the neutral plane is 0.35 in H₂O (88 Pa). This represents an extremely large fire, and the example is included to illustrate the extent to which equation (11) can be applied.

2.3 Expansion of Combustion Gases

In addition to buoyancy, the energy released by a fire can cause smoke movement due to expansion. In a fire compartment with only one opening to the building, air will flow into the fire compartment and hot smoke will flow out of the compartment. Neglecting the added mass of the fuel which is small compared to the airflow and considering the thermal properties of smoke to be the same as those of air, the ratio of the volumetric flows can be simply expressed as a ratio of absolute temperatures.

$$\frac{Q_{out}}{Q_{in}} = \frac{T_{out}}{T_{in}} \quad (12)$$

where:

- Q_{out} = volumetric flow rate of smoke out of the fire compartment
 Q_{in} = volumetric flow rate of air into the fire compartment
 T_{out} = absolute temperature of smoke leaving the fire compartment
 T_{in} = absolute temperature of air entering the fire compartment

For a smoke temperature of 1110 °F (600 °C), the gas will expand to about three times its original volume. For a fire compartment with open doors or windows, the pressure difference across these openings due to expansion is negligible because of the large flow areas involved. However, for a tightly constructed fire compartment without open doors or windows, the pressure differences due to expansion may be important.

2.4 Wind Effect

Wind can have an effect on smoke movement. The pressure, P_w , that wind exerts on a surface can be expressed as

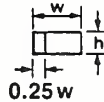
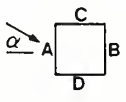

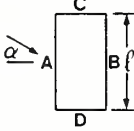

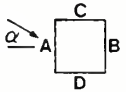

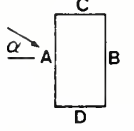
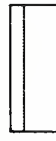
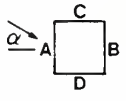

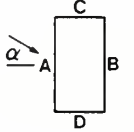
$$P_w = \frac{1}{2} C_w \rho_o U^2 \quad (13)$$

where C_w is a dimensionless pressure coefficient, ρ_o is the outside air density, and U is the wind velocity. Generally, the pressure coefficient, C_w , is in the range of -0.8 to 0.8, with positive values for windward walls and negative values for leeward walls. The pressure coefficient depends on building geometry and local wind obstructions, and the pressure coefficient varies locally over the wall surface. Values of pressure coefficient, \bar{C}_w , averaged over the wall area are listed in table 2 for rectangular buildings which are free of local obstructions.

The pressure difference from one side of a building to another due to wind effect can be expressed as

$$P_w = \frac{1}{2} (C_{w1} - C_{w2}) \rho_o U^2 \quad (14)$$

Table 2. Average pressure coefficients for walls of rectangular buildings
 [Adapted from MacDonald, (1975)]

Building Height Ratio	Building Plan Ratio	Elevation	Plan	Wind Angle α	\bar{C}_w for Surface			
					A	B	C	D
$\frac{h}{w} \leq \frac{1}{2}$	$1 < \frac{l}{w} \leq \frac{3}{2}$			0°	+0.7	-0.2	-0.5	-0.5
				90°	-0.5	-0.5	+0.7	-0.2
$\frac{1}{2} < \frac{h}{w} \leq \frac{3}{2}$	$\frac{3}{2} < \frac{l}{w} < 4$			0°	+0.7	-0.25	-0.6	-0.6
				90°	-0.5	-0.5	+0.7	0.1
	$1 < \frac{l}{w} \leq \frac{3}{2}$			0°	+0.7	-0.25	-0.6	-0.6
				90°	-0.6	-0.6	+0.7	-0.25
$\frac{3}{2} < \frac{h}{w} < 6$	$\frac{3}{2} < \frac{l}{w} < 4$			0°	+0.7	-0.3	-0.7	-0.7
				90°	-0.5	-0.5	+0.7	-0.1
	$1 < \frac{l}{w} \leq \frac{3}{2}$			0°	+0.8	-0.25	-0.8	-0.8
				90°	-0.8	-0.8	+0.8	-0.25
$\frac{3}{2} < \frac{l}{w} < 4$			0°	+0.7	-0.4	-0.7	-0.7	
			90°	-0.5	-0.5	+0.8	-0.1	

Note: h = height to eaves or parapet; l = length = the greater horizontal dimension of a building; w = width = the lesser horizontal dimension of a building

where the subscripts 1 and 2 refer to the windward and leeward sides of the building. Examples of wind induced pressures for wind speeds from 5 to 50 mph (2.24 to 22.4 m/s) are provided in table 1. Obviously, wind effects are most sever at high wind speeds and when windows are broken.

In general, wind velocity, U , increases with elevation, z , above the ground, as is expressed by the power law equation.

$$U = U_o \left(\frac{z}{z_o} \right)^n \quad (15)$$

where U_o is the velocity at elevation z_o , and n is the wind exponent. Wind data is recorded by airports and the weather service at heights, z_o , of about 33 ft (10 m) above the ground. This relationship has been extensively used to describe the velocity profile of the wind near the surface of the earth. It assumes that there are no large obstructions near the building that could produce local wind conditions. For buildings with such obstructions, specialized wind tunnel studies are needed to determine the pressure loadings due to the wind.

A value of 0.16 for the wind exponent is appropriate for flat terrain. The wind exponent increases with rougher terrain, and for very rough terrain, such as urban areas, a value of 0.40 is appropriate. In urban areas with a rather constant roof level, the wind gradient can be expressed as

$$U = U_o \left(\frac{z - y}{z_o} \right)^n \quad (15a)$$

Where y is the average roof height. Wind velocity profiles are illustrated in figure 6 for flat and very rough terrain. For further information about wind exponents and flow coefficients the reader is referred to texts on wind engineering such as those by Houghton and Carruthers (1976), Kolousek et al. (1984), MacDonald (1975), Sachs (1978), and Simiu and Scanlan (1986).

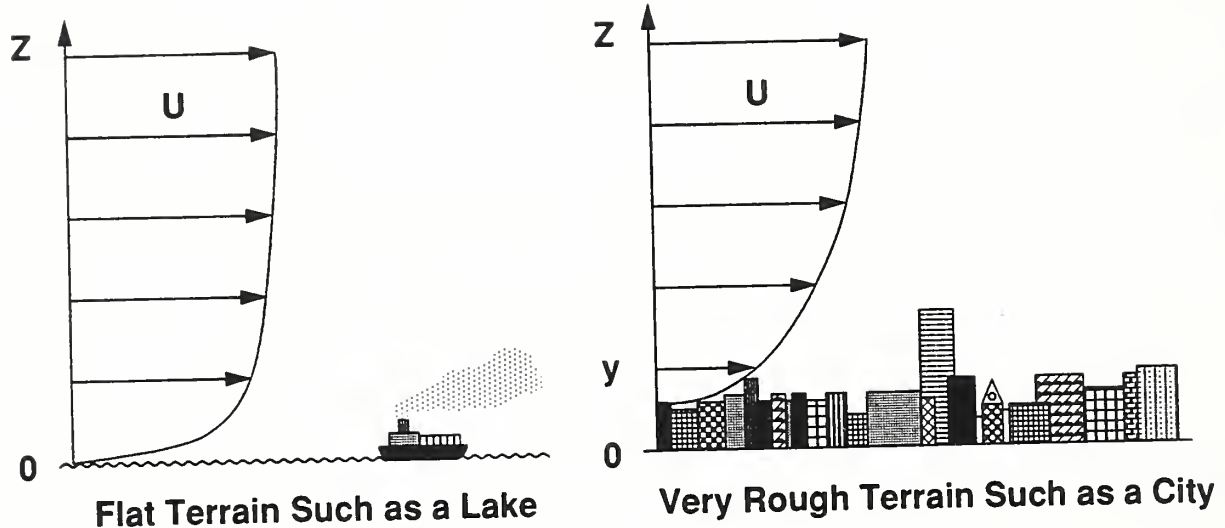


Figure 6. Wind velocity profiles for flat and very rough terrain

2.5 Ventilation Systems

Heating, ventilating and air conditioning (HVAC) systems frequently transport smoke during building fires. When a fire starts in an unoccupied portion of a building, the HVAC system can transport smoke to a space where people can smell the smoke and be alerted to the fire. Upon detection of fire or smoke, the HVAC system should be designed so that either the fans are shut-down or the system goes into a special smoke control mode of operation. The advantages and disadvantages of these approaches are complex, and no simple consensus has been reached regarding a preferred method for various building types. However, if neither fan shut-down nor smoke control is achieved, the HVAC system will transport smoke to every area the system serves. As the fire progresses, smoke in these spaces will endanger life, damage property and inhibit fire fighting. Although shutting down the HVAC system prevents it from supplying oxygen to the fire, system shut-down does not prevent smoke movement through the supply and return ducts, air shafts, and other building

openings due to stack effect, buoyancy, or wind. Computer simulation of smoke movement through HVAC systems are discussed by Klote (1987) and by Klote and Cooper (1988).

2.6 Elevator Piston Effect

When an elevator car moves in a shaft, transient pressures are produced. A downward-moving elevator car forces air out of the section of shaft below the car and into the section of shaft above the car as illustrated in figure 7. Klote and Tamura (1986) developed the following analytical equation for the pressure difference, ΔP_{s_o} , due to elevator piston effect between the outside and the elevator shaft above the car.

$$\Delta P_{s_o} = \frac{\rho}{2} \left[\frac{A_s U}{N_a C A_e + C_c A_f (1 + (N_a/N_b)^2)^{\frac{1}{2}}} \right]^2 \quad (16)$$

where:

- ρ = air density within the shaft
- A_s = cross-sectional area of shaft
- U = velocity of elevator car
- N_a = number of floors above the car
- N_b = number of floors below the car
- C = flow coefficient for building leakage paths
- A_e = effective flow area per floor between the shaft and the outside
- C_c = flow coefficient for flow around the car
- A_f = free flow area in shaft around car, or cross-sectional area of shaft less cross-sectional area of the car

The coefficient, C_c , was evaluated at 0.94 for a two car shaft with only one car moving and at 0.83 for a two car shaft with both cars traveling side-by-side together. The value for the two cars moving together is believed to be appropriate for obtaining approximations of pressures produced by the motion of a car in a single car shaft. For the sake of simplicity in the

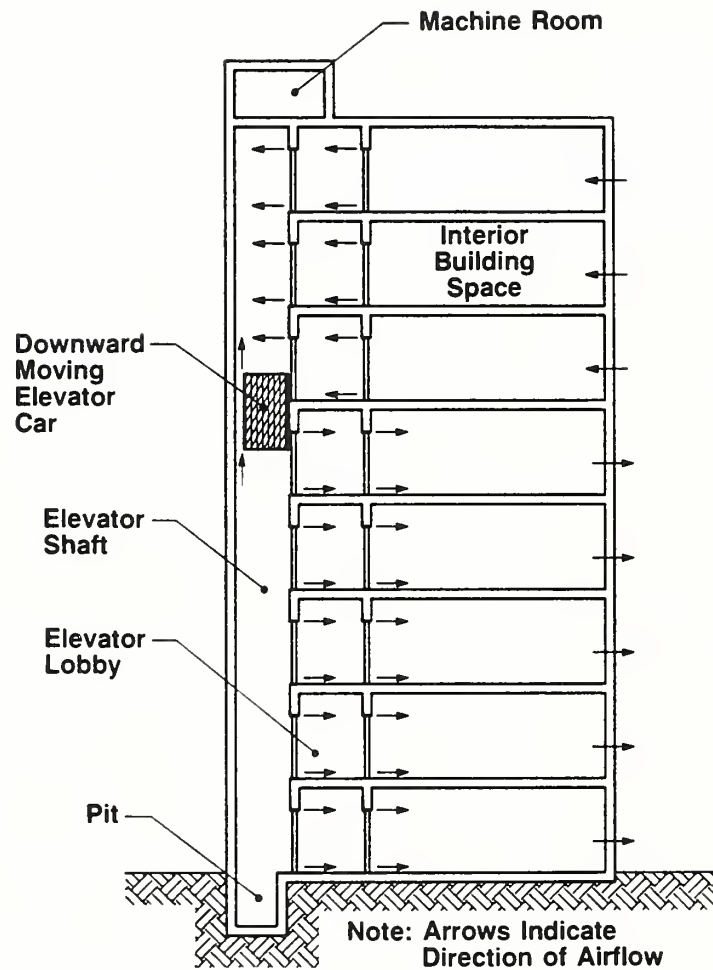


Figure 7. Airflow due to downward movement of elevator car

analysis leading to equation (16), buoyancy, wind, stack effect, and effects of the heating and ventilating system were omitted. Omitting stack effect is equivalent to stipulating that the building air temperature and the outside air temperature are equal.

For the system of three series flow paths from the shaft to the outside illustrated in Fig. 1, the effective flow area, A_e , per floor is

$$A_e = \left[\frac{1}{A_{1s}^2} + \frac{1}{A_{i1}^2} + \frac{1}{A_{oi}^2} \right]^{-\frac{1}{2}} \quad (17)$$

where A_{1s} is the leakage area between the lobby and the shaft, A_{i1} is the leakage area between the building and the lobby, and A_{oi} is the leakage area between the outside and the building. In a similar manner to the development for stack effect, the pressure difference, ΔP_{1i} , can be expressed as

$$\Delta P_{1i} = \Delta P_{so} (A_e/A_{1i})^2 \quad (18)$$

This series flow path analysis does not include the effects of other shafts such as stairwells and dumbwaiters. Provided that the leakage of these other shafts is relatively small compared to A_{oi} , equation (17) is appropriate for evaluation of A_e for buildings with open floor plans. Further, equation (18) is appropriate for closed floor plans, provided all the flow paths are in series and there is negligible vertical flow in the building outside the elevator shaft. The complicated flow path systems probably require case by case evaluation which can be done by using the effective area techniques presented in the ASHRAE smoke control manual (Klote and Fothergill 1983).

To test the above theory, experiments were conducted in a hotel in Toronto, Ontario, Canada. Figure 8 shows measured pressure differences across the top floor elevator lobby while a car was descending. Also shown is the calculated pressure difference which is in good agreement with the measurements. This experiment is described in detail by Klote and Tamura (1986). The pressure difference, ΔP_{1i} , can not exceed the upper limit of

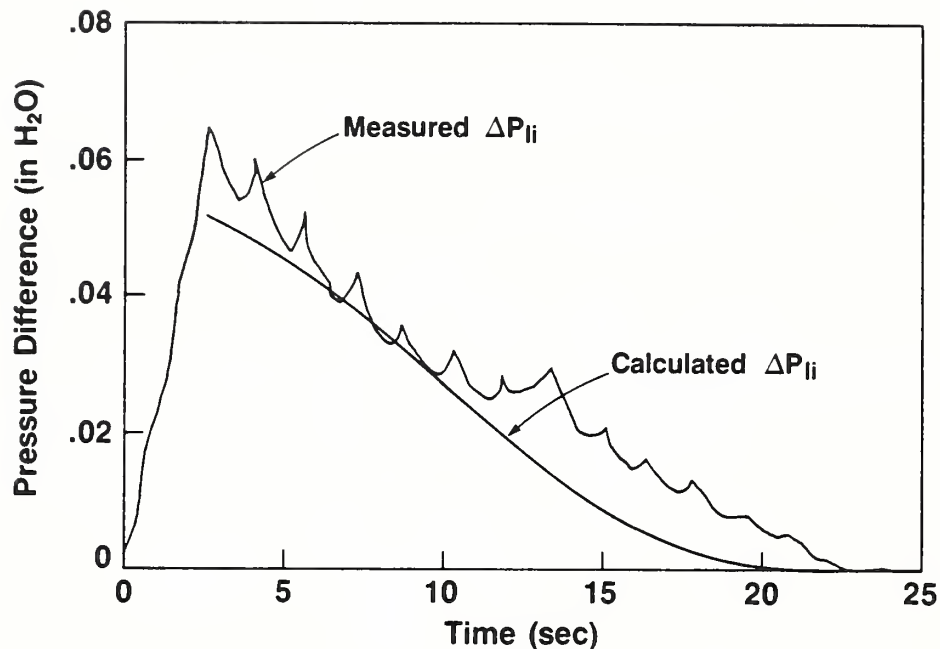


Figure 8. Pressure difference, ΔP_{1i} , across elevator lobby of a Toronto hotel due to piston effect

$$(\Delta P_{1i})_u = \frac{\rho}{2} \left[\frac{A_s A_e U}{A_f A_{i1} C_c} \right]^2 \quad (19)$$

where the subscript u denotes the upper limit. This relation is for unvented elevator shafts, or for which the vents are closed. The pressure difference, $(\Delta P_{1i})_u$, is strongly dependant upon U, A_s and A_f . For example, figure 9 shows the calculated relationship between $(\Delta P_{1i})_u$ and U due to one car moving in a single car shaft, a double car shaft and a quadruple car shaft. As expected the $(\Delta P_{1i})_u$ is much greater for the single car shaft. It follows that the potential for smoke problems due to piston effect in single car shafts is much greater than in multiple car shafts. Comparison of stack effect induced

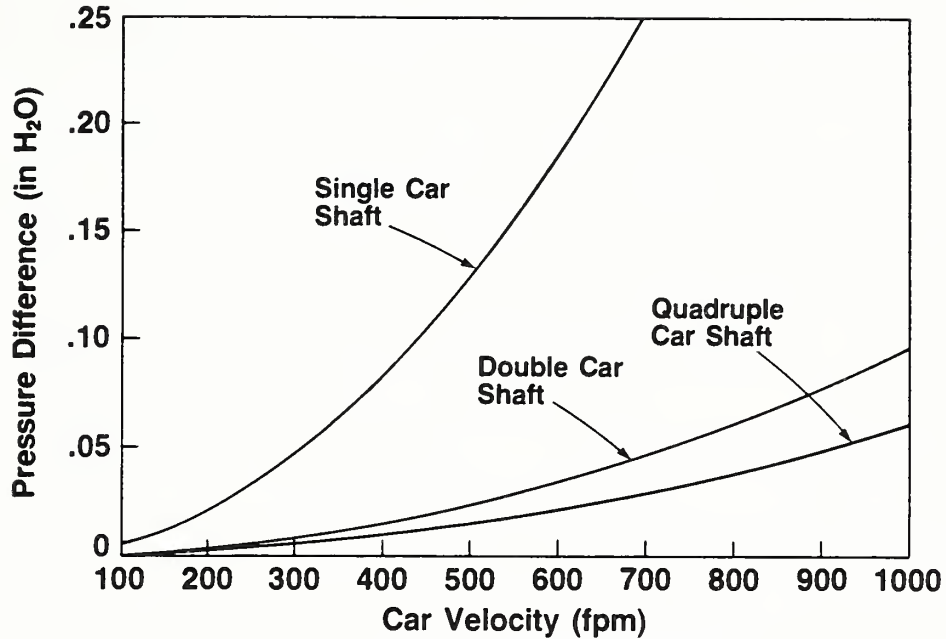


Figure 9. Calculated upper limit of the pressure difference, $(\Delta P_{1i})_u$, from the elevator lobby to the building due to piston effect

pressure differences indicates that they can be larger than those of other driving forces (table 1).

Operation of elevators by the fire service during a fire can result in smoke being pulled into the elevator shaft by piston effect. It seems a safe recommendation that fire fighters should favor the use of elevators in multiple car shafts over ones in single car shafts. Klote (1988a) developed another analysis of piston effect including the influence of elevator smoke control, and experiments conducted by Klote and Tamura (1987) were in good agreement with this theory.

3. LOCATION OF NEUTRAL PLANE

In this section methods of determining the location of the neutral plane are described for a single shaft connected to the outside only. The methods of effective area can be used to extend this analysis to buildings. Using these neutral plane locations, the flow rates and pressures throughout the building can be evaluated to the extent that the series flow model of section 2.1 is applicable.

3.1 Shaft with a Continuous Opening

The flow and pressures of normal stack effect for a single shaft connected to the outside by a continuous opening of constant width from the top to the bottom of the shaft is illustrated in figure 10. The following

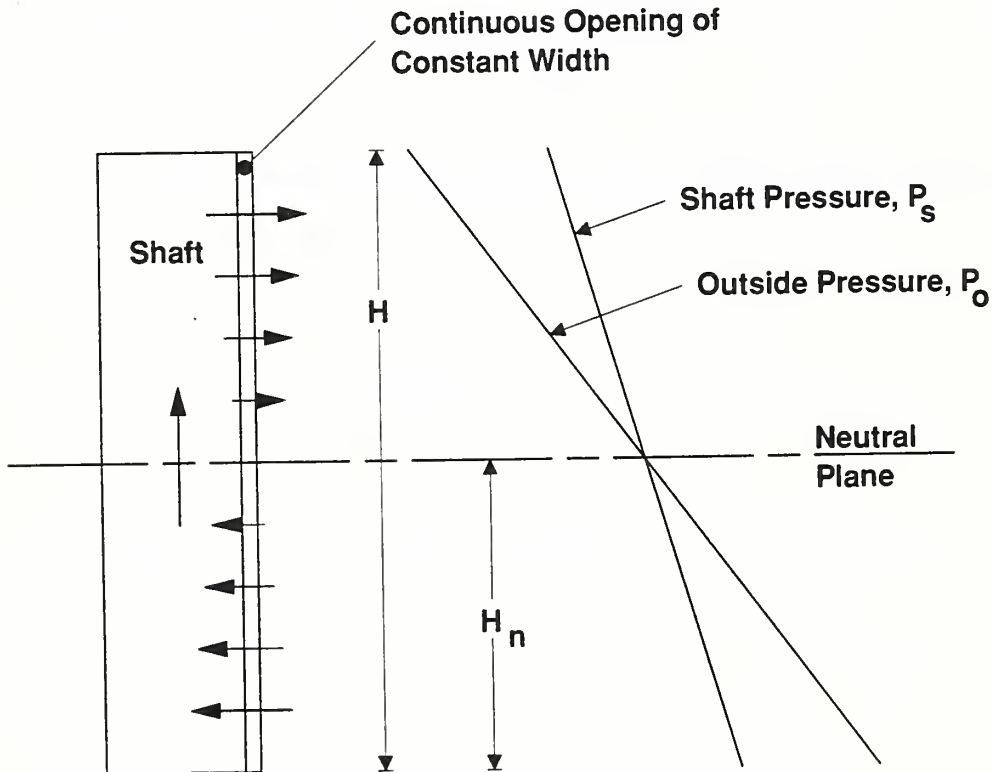


Figure 10. Normal stack effect between a single shaft connected to the outside by a continuous opening

analysis of this flow and the resulting location of the neutral plane was developed by McGuire and Tamura (1975). The pressure difference from the shaft to the outside is expressed by equation (6). The mass flow rate, dm_{in} , through the a differential section, dh , of the shaft below the neutral plane is

$$dm_{in} = C A' \sqrt{2 \rho_o \Delta P_{s_o}} dh = C A' \sqrt{2 \rho_o b h} dh \quad (20)$$

where

$$b = \frac{g P_{atm}}{R} \left(\frac{1}{T_o} - \frac{1}{T_s} \right)$$

and where A' is the area of the opening per unit height. To obtain the mass flow rate into the shaft, this equation can be integrated from the neutral plane ($h = 0$) to the bottom of the shaft ($h = -H_n$).

$$m_{in} = \frac{2}{3} C A' H_n^{3/2} \sqrt{2 \rho_o b} \quad (21)$$

In a similar manner an expression for the mass flow rate from the shaft can be developed, where H is the total height of the shaft.

$$m_{out} = \frac{2}{3} C A' (H - H_n)^{3/2} \sqrt{2 \rho_s b} \quad (22)$$

For steady flow, the mass flow rate into the shaft equals that leaving it. Equating equations (21) and (22), cancelling like terms, rearranging, and substituting equation (5) yields

$$\frac{H_n}{H} = \frac{1}{1 + (T_s/T_o)^{1/3}} \quad (23)$$

For an inside temperature of 72 °F (22 °C) and an outside temperature of 0 °F (-18 °C), the neutral plane is located 48.8 percent up the height of the shaft which is slightly different from the generally accepted approximation of halfway up the shaft.

3.2 Shaft With Two Vents

Normal stack effect for a shaft with two openings is illustrated in figure 11. The pressure difference from the shaft to the outside is expressed by equation (6). To simplify analysis, the distance, H , between the openings is considered much greater than the height of either opening. Thus the

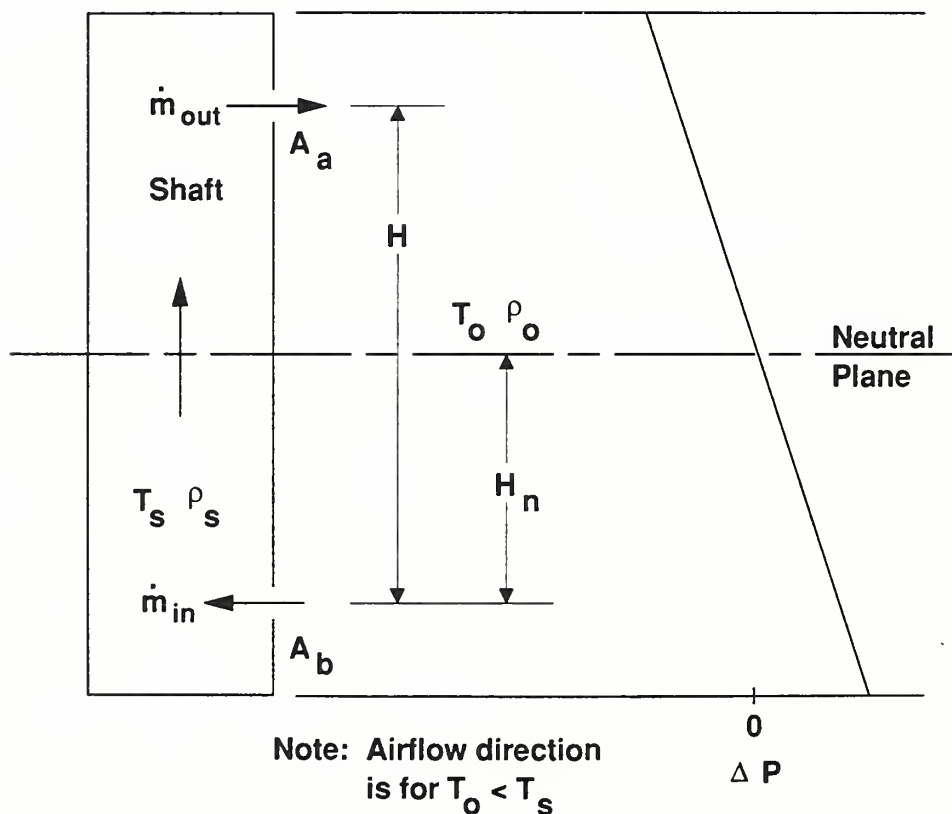


Figure 11. Stack effect for a shaft with two openings

variation of pressure with height for the openings can be neglected, and the mass flow rate into the shaft can be expressed as

$$m_{in} = C A_b \sqrt{2 \rho_o b H_n} \quad (24)$$

and the mass flow rate out of the shaft is

$$m_{out} = C A_a \sqrt{2 \rho_s b (H - H_n)} \quad (25)$$

Where A_a and A_b are the areas above and below the neutral plane. Equating these two flows as was done above yields

$$\frac{H_n}{H} = \frac{1}{1 + (T_s/T_o)(A_b/A_a)^2} \quad (26)$$

For an inside temperature of 72 °F (22 °C), an outside temperature of 0 °F (-18 °C), and equal areas ($A_b = A_a$), the neutral plane is located 46.4 percent up the height of the shaft which is only a little less than the case of the continuous opening (48.8 percent). The location of the neutral plane is highly dependant on the ratio A_b/A_a . For A_b/A_a that approaches zero, H_n approaches H. This means that if the area at the bottom is very small compared to the area at the top, then the neutral plane is at or near the top area. Equation (26) is a strong function of the flow areas and a weak function of temperature.

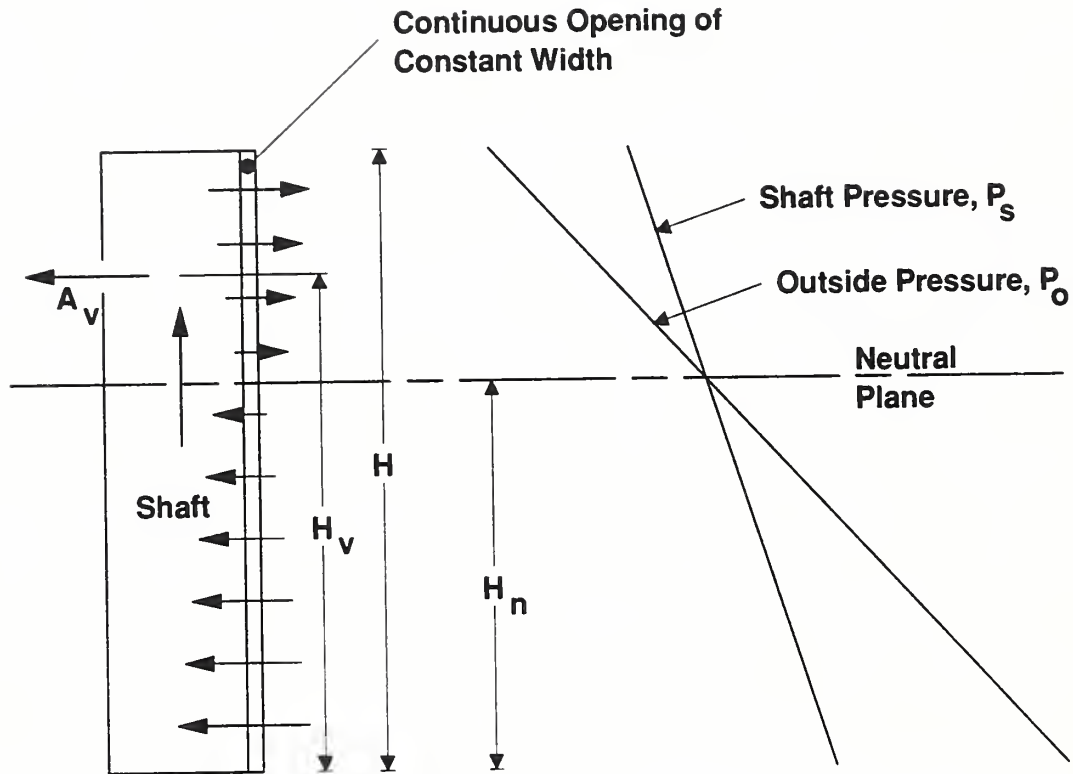


Figure 12. Normal stack effect between a single shaft connected to the outside by a vent and a continuous opening

3.3 Vented Shaft

The flow and pressures of normal stack effect for a shaft connected to the outside by a vent and a continuous opening are shown in figure 12. The following analysis is for a vent above the neutral plane, but a similar one can be made for a vent below the neutral plane. This analysis is an extension of one by McGuire and Tamura (1975) for a top vented shaft. The mass flow into the shaft is expressed by equation (21). For simplicity of analysis, the height of the vent is considered small in comparison to the shaft height, H . Thus, a constant pressure difference can be used to describe the flow through

the vent. The mass flow out of the shaft is the sum of the flow out of the continuous opening, expressed as equation (22), plus the flow out of the vent of area A_v located at an elevation of H_v above the shaft bottom.

$$m_{out} = \frac{2}{3} C A' (H - H_n)^{3/2} \sqrt{2 \rho_s b} + C A_v \sqrt{2 \rho_s b (H_v - H_n)} \quad (27)$$

Continuity of mass equation for the shaft can be written as

$$\begin{aligned} \frac{2}{3} C A' (H - H_n)^{3/2} \sqrt{2 \rho_s b} + C A_v \sqrt{2 \rho_s b (H_v - H_n)} = \\ \frac{2}{3} C A' H_n^{3/2} \sqrt{2 \rho_o b} \end{aligned} \quad (28)$$

Cancelling like terms and incorporating equation (5) results in

$$\frac{2}{3} A' (H - H_n)^{3/2} + A_v (H_v - H_n)^{1/2} = \frac{2}{3} A' H_n^{3/2} (T_s/T_o)^{1/2} \quad (29)$$

As would be expected, this equation reduces to equation (23) for $A_v = 0$. Equation (29) can be rearranged as

$$\frac{2 A' H (H - H_n)^{3/2}}{3 A_v H} + \frac{(H_v - H_n)^{1/2}}{H} - \frac{2 A' H H_n^{3/2} T_s^{1/2}}{3 A_v H T_o^{1/2}} = 0 \quad (30)$$

For relatively large vents, the ratio $A'H/A_v$ approaches zero. As $A'H/A_v$ approaches zero, the first and third terms in the above equation approach zero, and the equation is reduced to $H_n = H_v$. Thus the neutral plane is at or near the vent elevation, for a vent area very much greater than the area of the continuous opening ($A'H$). As with equation (26), the above equation is a strong function of the flow areas and a weak function of temperature.

Regardless of whether the vent is above or below the neutral plane, the neutral plane will be located between the height described by equation (23) for an unvented shaft and the vent elevation, H_v . Further, the smaller the value of $A'H/A_v$, the closer the neutral plane will be to H_v .

4. FRICTION LOSS IN SHAFTS

In the discussions above, the pressure losses due to friction in shafts were assumed negligible. If the flow rate in a shaft is relatively small, this assumption is appropriate. However, for high flow rates in shafts, friction losses can be significant. For straight shafts such as elevator shafts, the friction loss, ΔP_f , is expressed by the Darcy equation

$$\Delta P_f = f \frac{L}{D_e} \rho \frac{U^2}{2} \quad (31)$$

where f is the friction factor, L is the length of the duct, D_e is the effective diameter of the duct, ρ is the density of the gas in the duct, and U is the average velocity in the duct. Incorporation of the effective diameter allows evaluation of ducts with various geometries, and the reader is referred to the ASHRAE Handbook (1985) for a discussion of effective diameters. The friction factor is a function of the Reynolds number and the relative roughness of the duct, and it can be obtained from the well known friction factor diagrams reproduced in most elementary fluid dynamics texts. For calculations of losses in shafts, the flow is approximated as a function of mass flow rate, m , in the shaft by Klote and Fothergill (1983) as

$$\Delta P_f = (m/C_s)^2 \quad (32)$$

where

$$C_s = \sqrt{\frac{2 D_e \rho A^2}{f L}}$$

for straight shafts with cross sectional area of A, and L is one floor height of the shaft. For stairwells the friction factor is nearly constant over the relevant range of flows, and C_s is approximated by a constant. C_s is dependant on the cross sectional area, A, of the stairwell, and can be expressed as $C_s = C_s' A$ based on research of Tamura and Shaw (1976). An average value of $C_s' = 49 (.25)$ is recommended for area in ft^2 (m^2), pressure loss in inches H_2O (Pa) per floor, and mass flow rate in lb/min (kg/s). Based on the example analyses presented later in this paper, the flows due to stack effect in stairwells are on the order of:

lb/min (kg/s)		
60 (0.5)		with all doors closed and no vents, and
600 (4.6)		with a top vent and an exterior door open.

For a stairwell with a cross sectional area of 120 ft^2 (11 m^2), these flows result in the following pressure losses per floor:

in H_2O (Pa)		
0.0001 (0.025)		with all doors closed and no vents,
0.01 (2.5)		with a top vent and an exterior door open.

These losses can be compared to the pressure difference due to stack effect as expressed by equation (6). For an outside temperature of $0 \text{ }^\circ\text{F}$ ($-18 \text{ }^\circ\text{C}$), and an inside temperature of $72 \text{ }^\circ\text{F}$ ($22 \text{ }^\circ\text{C}$), the pressure due to stack effect is about 0.02 in H_2O (5 Pa) at one floor [10 ft (3 m)] above the neutral plane. A height of one floor was used so that the basis of comparison would be the same with the friction losses. These calculations indicate that pressure losses due to friction are generally negligible for shafts with all doors closed and no vents, but shaft friction can be significant for many common situations such as shafts with open doors or vents.

5. STEADY SMOKE CONCENTRATIONS

Tamura (1969) developed a simple method to calculate steady smoke concentrations, and this steady smoke approach is addressed here because it leads to an understanding of smoke flow under limited conditions. This model is based on the assumption of perfect mixing. That is, that the smoke concentration is uniform throughout a space, and consequently that mixing of flows into the space occurs instantly. This assumption is appropriate to the extent that the air in the room is well mixed due to the effect of a ventilation system, motion of people, room air currents due to convective heat transfer, cooling fans in electronic equipment, or other effects. Zone models addressed later do not have this limiting assumption.

The mass flow rate of a substance into a space equals the mass flow rate of that substance out of the space. For a building space i , this mass balance relation can be expressed as

$$\sum_j (m_{ij} c_j)_{in} = \sum_j (m_{ji} c_i)_{out} \quad (33)$$

where c_i and c_j are the concentrations in spaces i and j respectively, and the subscripts in and out indicate flow into and out of space i respectively. This equation can be solved for the smoke concentration of space i

$$c_i = \sum_j (m_{ij} c_j)_{in} / \sum_j (m_{ji})_{out} \quad (34)$$

For a number of informative cases, the pressures and mass flow rates can be calculated as discussed above, and equation (34) can be used to determine the steady smoke concentrations. Such calculations of mass flow rate are time consuming and limited to a few simple cases of building leakage conditions. However, the computer models to calculate air these flows are addressed in the next section.

6. NETWORK MODELS

The above methods for determination of neutral plane are limited to a few simple geometries. A number of network computer models have been developed that can be used to analyze flows and pressures in buildings with very complicated flow systems. It should be noted that these network models differ from zone models which are discussed later. This section provides an overview of these programs. Because of the number of programs involved, an exhaustive cataloging of network models is beyond the scope of this paper. However, Feustel and Kendon (1985) at Lawrence Berkeley Laboratory have prepared a literature review of network models used for air flow analysis in buildings, and Said (1988) of the National Research Council of Canada has evaluated several such models with respect to applicability for smoke control analysis.

Some computer programs only simulate airflow in buildings such as the ventilation models of Sander and Tamura (1973) and Sander (1974) and the smoke control model by Klote (1982). Other programs model smoke movement within a building such as ones by Butcher, et al. (1969), Barrett and Locklin (1969), Wakamatsu (1977), Evers and Waterhouse (1978), and Yoshida et al. (1979). Some programs include extensive heat transfer algorithms such as the Thermal Analysis Research Program (TARP) by Walton (1984).

6.1 Network Model Concept

In all the above computer programs, a building is represented by a network of spaces or nodes, each at a specific pressure and temperature. Vertical shafts such as stairwell, elevator shafts, mail chutes, dumbwaiters, mechanical shafts, and electrical shafts are modeled by a series of vertical spaces, one for each floor. Air flows through openings from regions of high pressure to regions of low pressure. These flow paths may be open windows or doors, gaps around interior doors, or very narrow cracks around weatherstripped windows and doors. Less obvious but no less important leakage paths are construction cracks, such as where walls meet floors, where ceiling tiles meet a steel suspension grid, where walls interface with window frames and door frames, around electrical fixtures and outlets, and at plumbing fixtures. Air flow through these paths is a function of the pressure difference across the path and the path geometry. Outside pressures incorporate the effects of air temperature and wind. The building's heating, ventilating and air conditioning (HVAC) systems are also taken into account.

In the smoke movement models, smoke generated in the fire compartment flows through openings to adjacent spaces and is carried along with building air currents through complex paths to locations remote from the fire. In some of the models, the temperature of spaces increases due to the flow of hot smoke, while heat is transferred from the smoke to the building's interior surfaces.

Each network model is to some extent unique, depending on its intended application. However, the computer programs are similar in many respects, and the equations provided in the following sections form a general description of this class of model.

6.2 Mass Flow Rates

For the same conditions of pressure and temperature, there are negligible differences in fluid properties between clean air and smoke.

Consequently, the network smoke movement models calculate only air flows, and as the need arises, smoke concentrations in air are evaluated. Accordingly, the air movement portion of the program can be described by the same equations that describe air movement for ventilation or energy analysis programs.

The mass flow rate, $m_{i,j}$, to space i from space j through a flow path with cross-sectional area $A_{i,j}$ is expressed by the flow equation

$$m_{i,j} = S C A_{i,j} \sqrt{2\rho |P_j - P_i|} \quad (35)$$

where P_i and P_j are the pressures of spaces i and j , respectively, S is the sign of $(P_j - P_i)$, and C is the flow coefficient. Generally, space j is another location within the building, however, it can be outside the building. An outside pressure P_j is dependent on outside air temperature and wind effects. Considerable data concerning building air leakage is provided in the ASHRAE Handbook of Fundamentals (1985, Chapter 22). Typical leakage areas of construction cracks in walls and floors of commercial buildings have been tabulated by Klote and Fothergill (1983, Appendix C). Strictly speaking, network models have the limitation that flow between two spaces can only be in one direction. However, some of these models allow bidirectional flow in the vicinity of the fire. For a building space i , the mass balance equation is

$$\sum_j m_{i,j} = 0 \quad (36)$$

In general, the mass flows are described by equation (35), however, the effects of ventilation systems can be expressed by incorporating a constant flow term from a ventilation space j .

By substitution of equation (35) into equation (36) and expressing in terms of space pressure, a system of equations can be obtained for all n spaces of a building network.

$$\begin{aligned}
m_1 (P_1, P_2, \dots, P_n) &= 0 \\
\vdots & \\
m_i (P_1, P_2, \dots, P_i, \dots, P_n) &= 0 \\
\vdots & \\
m_n (P_1, P_2, \dots, P_n) &= 0
\end{aligned}
\tag{37}$$

Thus the building pressures, P_1 to P_n , are solved simultaneously by solving n number of mass balance equations. In reality, the number of pressures included in an equation $m_i = 0$ are only P_i and those pressures of spaces directly connected to space i . Because each of the equations is nonlinear as represented by equation (35), it is generally difficult to solve these systems of equations in an analytical way. A discussion of the numerical techniques involved is beyond the scope of this paper. However, this problem is mathematically similar to the analysis of water flow in piping networks the computer solution of which the civil engineering community has had considerable success. Wood and Rayes (1981) have evaluated several commonly used algorithms for the water flow networks.

6.3 Unsteady Smoke Concentrations

As with the method for calculating steady smoke concentrations, simulation of unsteady smoke flow in network models is based on the perfect mixing assumption. At an arbitrary time, $t = k \Delta t$ ($k = 0, 1, 2, \dots$) where Δt is a time interval, the balance of concentrations for space i is

$$\left[\sum_j (m_{ij} c_j)_{in} - \sum_j (m_{ji} c_i)_{out} \right] \Delta t = V_i \rho_i \Delta c_i
\tag{38}$$

where V_i is the air volume of space i , c_i and c_j are concentrations in spaces i and j , respectively, and Δc_i is the change of concentration within space i during the time interval. The change in concentration can be expressed as $\Delta c_i = c_i(k+1) - c_i(k)$, where k refers to time steps. From equation (36) the following equation for the concentration in space i was derived by Wakamatsu (1977)

$$c_i(k+1) = \frac{SMc_i}{SM_i} + (c_i(k) - SMc_i/SM_i) \exp\left[-\frac{SM_i \Delta t}{V_i \rho_i}\right] \quad (39)$$

where

$$SMc_i = \sum_j [m_{ij}(k) c_j(k)]_{in}$$

and

$$SM_i = \sum_j [m_{ji}(k)]_{out}$$

Thus the concentrations, c_i , at time step $k+1$ can be calculated in terms of the concentrations and mass flow rates at time step k . The concentration in the fire compartment is the driving force, and many models like Wakamatsu (1977) and Evers and Waterhouse (1978) assume that the fire compartment concentration is constant throughout the fire. The whole fire space is assumed at a uniform temperature. This can be thought of as modelling smoke movement due to smoldering fire or, neglecting early fire growth, smoke movement due to an intense fire that exists when a compartment is fully involved in fire. The model by Yoshida et al. (1979) accepts a user defined time profile of smoke concentration and temperature of the fire compartment.

A significant shortcoming of the network smoke movement models is their treatment of the fire compartment and spaces directly connected to it. In these spaces smoke generally is not perfectly mixed, but forms a hot upper layer. Whenever, a gas flows into a compartment in which the gas has some buoyant force, there is a tendency toward forming an upper layer. The extent to which the forces promoting mixing (ventilation systems, convection currents, etc.) interfere with smoke stratification is unknown. Research is needed to develop an understanding of smoke movement far from the fire source. Network models should be used with caution concerning their particular assumptions and the limitations of knowledge in this entire area.

6.4 Unsteady Temperatures

Network models for building energy analysis, such as TARP (Walton 1983) simulate heat transfer in considerable detail including solar gains through windows, walls and roof, as well as, heat transferred between interior building components by conduction, convection and radiation. It should be noted that the energy models calculate flows and temperatures at one to three hour intervals which is inappropriate for simulation of building fires. Wakamatsu handles convective heat transfer, and calculates unsteady temperatures for building spaces. However, most of the ventilation models such as Sander and Tamura (1973) and some of the smoke movement models such as Evers and Waterhouse (1978) and Yoshida et al. (1979) assume constant, user defined temperatures throughout the building. This can be appropriate for ventilation models applied to buildings that have heating and cooling systems to maintain nearly constant temperatures. It is probably appropriate for simulation of smoke movement due to a smoldering fire. While the constant temperature assumption is unrealistic with respect to flaming fires, it still can be used to gain some insight into gross smoke movement in large buildings.

7. ZONE MODELS

The common feature of zone fire models is that they describe the bulk of a room's fire-generated environment, away from fire plumes and near-surface boundary flows, as being divided into two uniform-property zones: an upper layer of 'hot' air, heavily contaminated with the fire's products of combustion, i.e., the smoke, and a lower layer of relatively uncontaminated and relatively cool air. Examples of zone models are those by Zukoski and Kubota (1980), Mitler and Emmons (1981), Quintiere, et al. (1981), Cooper (1982), Tanaka (1983), and Jones (1985). A comparison of the various models is beyond the scope of this paper. However, the mathematical framework of each of these models has much in common with the others as is obvious from the review of zone models by Jones (1983). Further, Mitler (1985) compares the features of three of these fire models.

The intent of this section is to provide a simple description of zone models in order to show the potential of these models in addressing smoke movement in buildings due to stack effect. It should be realized that each model has its own level of detail and its own unique assumptions in describing mathematically the processes of combustion, heat and mass transfer, and flow dynamics. The following, adopted from Klote and Cooper (1988), is a brief generic description of compartment fire phenomena and of the class of zone-type compartment fire models of these phenomena. For more extensive discussions of the overall phenomena the reader is referred to Cooper (1984) and Kennedy and Cooper (1987) for qualitative aspects and to the above-referenced model references for quantitative aspects.

7.1 Compartment Fire Phenomena

Refer to Figure 13. In a room of fire involvement, air which supports the combustion process is entrained into the combustion zone and mixes with combustion products. There the mixture of gases and fire-generated particulates are heated and driven upward. These materials form a buoyant plume which continues to entrain and mix with air and cool as it rises above the combustion zone to the ceiling. A portion of the energy released from the combustion zone is transferred by radiation to the walls, floor and ceiling.

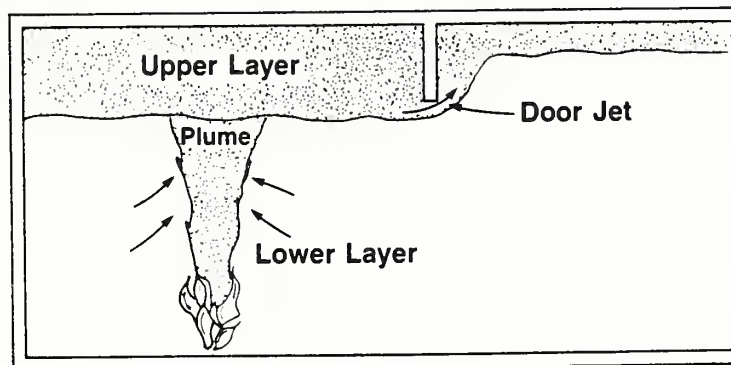


Figure 13. Stratified smoke flow as simulated by zone fire models

As a result of this, the temperature of these materials begin to increase.

As the plume impinges on the ceiling it is redirected outward as a relatively high temperature radial ceiling jet which heats by convection the ceiling surface. Having reached the bounding walls of the room, the buoyant plume gases and particulates eventually redistribute themselves across the entire upper portion of the room and begin to form a relatively quiescent, elevated-temperature smoke layer. As the plume continues to entrain air from the lower portion of the room and to add new material to upper portion of the room the smoke layer grows in thickness and changes in composition.

The interface which separates the upper smoke layer from the lower air layer typically drops eventually below the tops of doors, windows, or other open vents. The smoke then flows out of the fire room and into adjacent rooms or into the atmosphere. At a given vent this outward flow is often exchanged and mixed with inward flowing fresh air. These multi-directional vent flows are driven by room-to-room, cross-vent, hydrostatic pressure differences which vary as a function of elevation and which can change sign one or more times across the vertical extent of a vent.

High temperature smoke which enters an adjacent space is relatively buoyant there and rises to the ceiling by buoyant flow processes which are reminiscent of those discussed above for the fire plume. For example, as illustrated in Figure 13, upper layer gases flowing through a doorway can form an upward flowing door jet, which can begin to form and then add to the growth of an upper layer in an adjacent room. Thus, smoke-filling and -transport is initiated in the adjacent spaces of the facility and beyond.

As mentioned, the major assumption of zone models is that they simulate the fire-generated environment in each room as being divided into an upper, elevated-temperature smoke layer and a lower, relatively-cool, and less-contaminated air layer. This is illustrated in Figure 13.

For simplification, the temperature and composition of each layer is considered homogeneous. In the bulk of the room, away from plumes, vent-

flows, and near-surface boundary flows, the environment is relatively quiescent and the pressure, P , is estimated by hydrostatics, i.e., $P = \int g\rho dz$, where g is the acceleration of gravity, ρ is the density, and z is elevation. A Bernoulli-equation formulation of the momentum equation and z -dependent, cross-vent, pressure differences are used to compute the z -dependent velocity of room-to-room mass exchanges. Rules for depositing the vent flows into the upper or lower layer of the receiving room are established.

The upper and lower layer of each room is required to satisfy conservation of mass, energy, and species and the equation of state. This leads to a set of time-dependent differential equations in the independent variables. These are the variables which can be used to describe completely the state of both layers, i.e., the overall fire environment, in the room. The equations for all rooms of a simulation taken together form the complete equation set for the model.

The following equations, taken from the CCFM zone model formulation of Cooper and Forney (1987), is an example of a fully-general set of equations for an arbitrary room of a simulation. They are given in the independent variables p , pressure at the floor of the room; V_U , volume of the upper layer; ρ_U and ρ_L , densities of the upper and lower layer; and $c_{i,U}$ and $c_{i,L}$, concentration of product of combustion i in the upper and lower layer. The equations for the dependent variables, T_U and T_L , the temperatures of the upper and lower layers, are also shown. As can be seen below, these are obtained directly from the equation of state of a perfect gas, which is assumed traditionally to be a useful approximation in zone fire model formulations. The complete set of equations is valid when the layer interface is between the floor and the ceiling of the room, i.e., whenever $0 < V_U < V$, the volume of the room.

pressure at the floor of the room:

$$dP/dt = [(\gamma - 1)/V](q_L + q_U)$$

volume of the upper layer:

$$dV_U/dt = [(\gamma - 1)/(\gamma P)][(1 - V_U/V)q_U - (V_U/V)q_L]$$

densities of the upper and lower layer:

$$d\rho_U/dt = (1/V_U)(m_U - \rho_U dV_U/dt)$$

(40)

$$d\rho_L/dt = [1/(V - V_U)](m_L + \rho_L dV_U/dt)$$

concentration of product of combustion i in the upper and lower layer:

$$dc_{i,U}/dt = [1/(\rho_U V_U)](M_{i,U} - m_U c_{i,U})$$

$$dc_{i,L}/dt = \{1/[\rho_L (V - V_U)]\}(M_{i,L} - m_L c_{i,L})$$

absolute temperature of the upper and lower layer:

$$T_U = P/(\rho_U R); \quad T_L = P/(\rho_L R)$$

Beside the independent variables and the physical constants γ , ratio of specific heats, and R , the gas constant, the right-hand-side of the above equations depend only on: q_U and q_L , the net rate of enthalpy plus heat transfer plus energy release flowing to the upper and lower layer; m_U and m_L , the net rate of mass flowing to the upper and lower layer; and $M_{i,U}$ and $M_{i,L}$, the net rate of product i flowing to the upper and lower layer. At any instant of time during the course of a fire simulation, the contributions to these terms are dependent on the details of the individual algorithms which describe mathematically the combustion and the various mass and heat transfer processes, e.g., the plume equations, rules for distributing vent flows into the two layers of the receiving room, and the equations for radiative exchanges.

In principle, the above equation set should contain the equation set of any zone-fire model. However, the type and sophistication of the solution

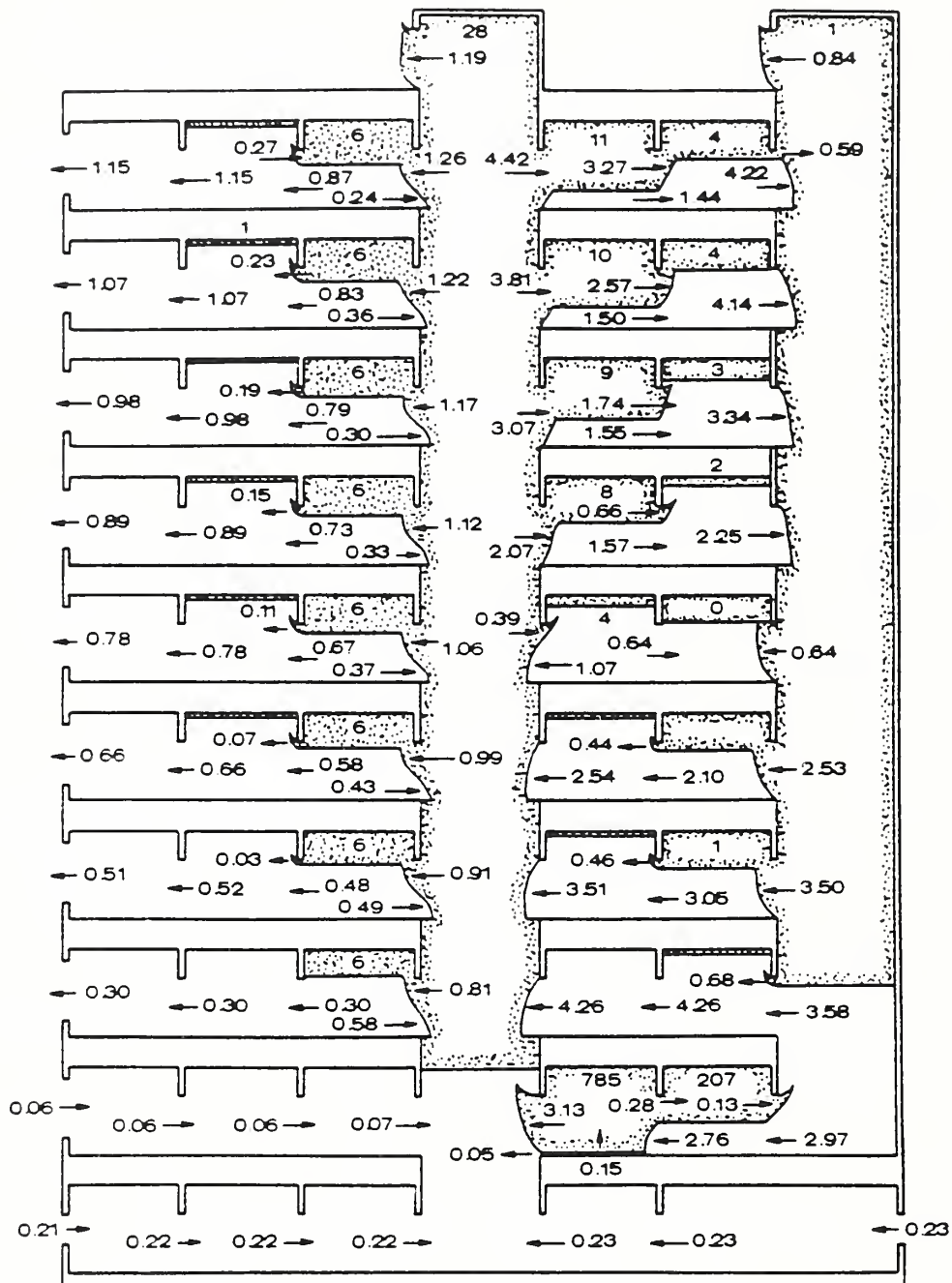
techniques that could be used, whether analytic or, more typically, numeric are not unique. Also, the actual form of (the right hand side of) these equations would depend on the particular details of the collection of algorithms which describe the individual physical phenomena. The CCFM will be relatively flexible with regard to choice of these details. It is being developed in a manner that will allow for a wide range of modeling detail, from basic to "benchmark" simulations.

7.2 Application to High Rise Buildings

Tanaka (1983) used a zone model to simulate smoke transport in large buildings, and figures 14 through 17 show his analysis of smoke conditions in a ten story building with two shafts at 0.5, 1.0, 3.0 and 4.5 minutes after ignition. Even though Tanaka's analysis did not include naturally occurring stack effect nor wind effect, this work is discussed here to show the capabilities of zone modelling with respect to large buildings. The dimensions of the rooms, shafts, interior openings and exterior openings for these analyses are listed in table 3. At 0.5 minutes (figure 14), both shafts for the most part have filled with smoke, and smoke is flowing out of the shafts on most floors. It should be noted that for most of the interior openings, the flow is bidirectional, and at some locations the flow is tridirectional. At 1.0 and 3.0 minutes (figures 15 and 16), the smoke spread and the temperatures of the upper layers have increased.

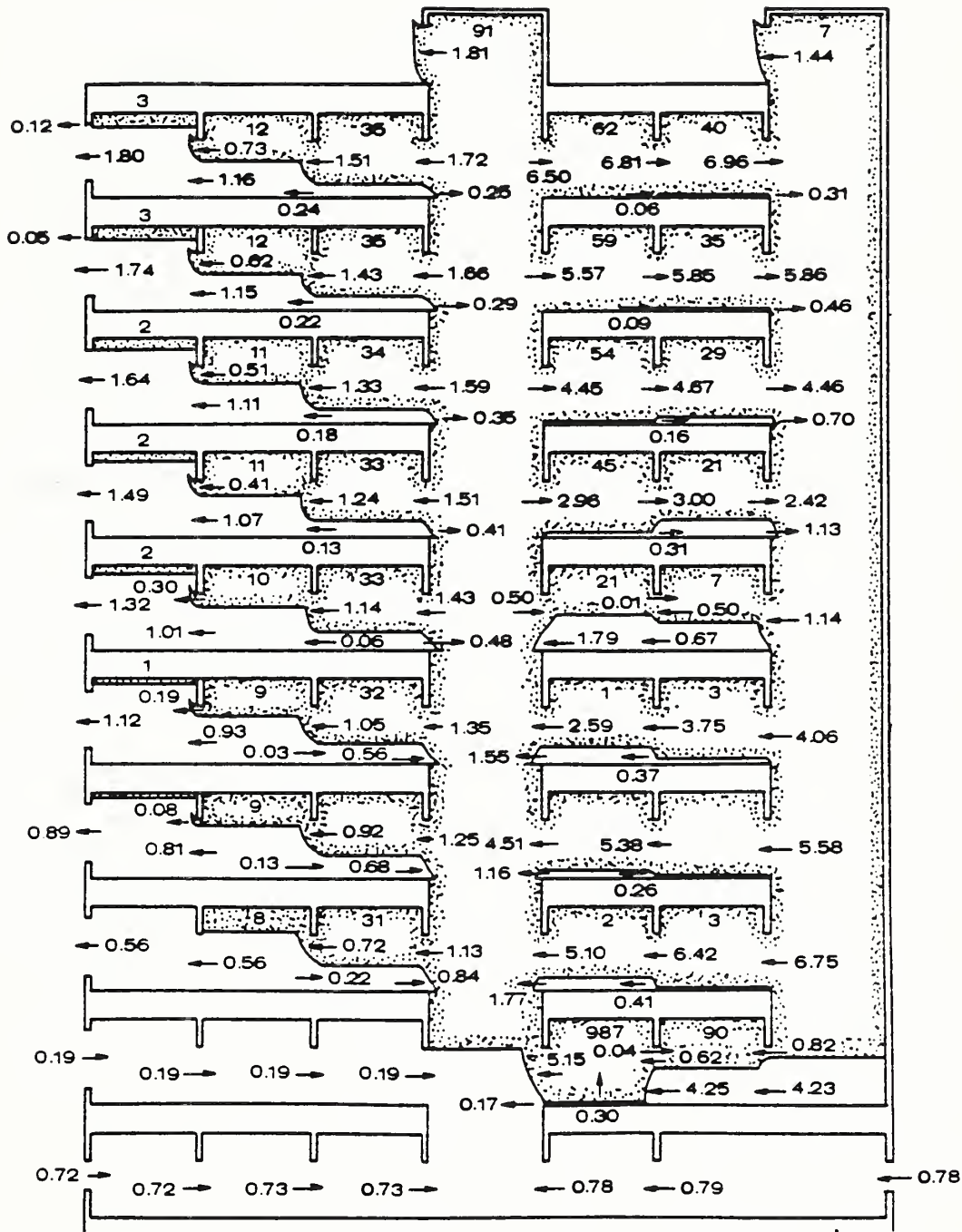
Table 3. Dimensions used for Tanaka's (1983) zone model simulation of smoke movement in a ten story building

Item	Dimensions
all rooms	13 x 20 x 9.8 ft high (4 x 6 x 3 m high)
1st shaft	13 x 20 x 139 ft high (4 x 6 x 42.5 m high)
2nd shaft	13 x 20 x 126 ft high (4 x 6 x 38.5 m high)
exterior opening on 1st floor	3.3 x 3.3 ft (1 x 1 m).
exterior openings on other floors	0.33 x 3.3 ft high (0.1 x 1 m high)
interior openings	3.3 x 6.6 ft high (1 x 2 m high)



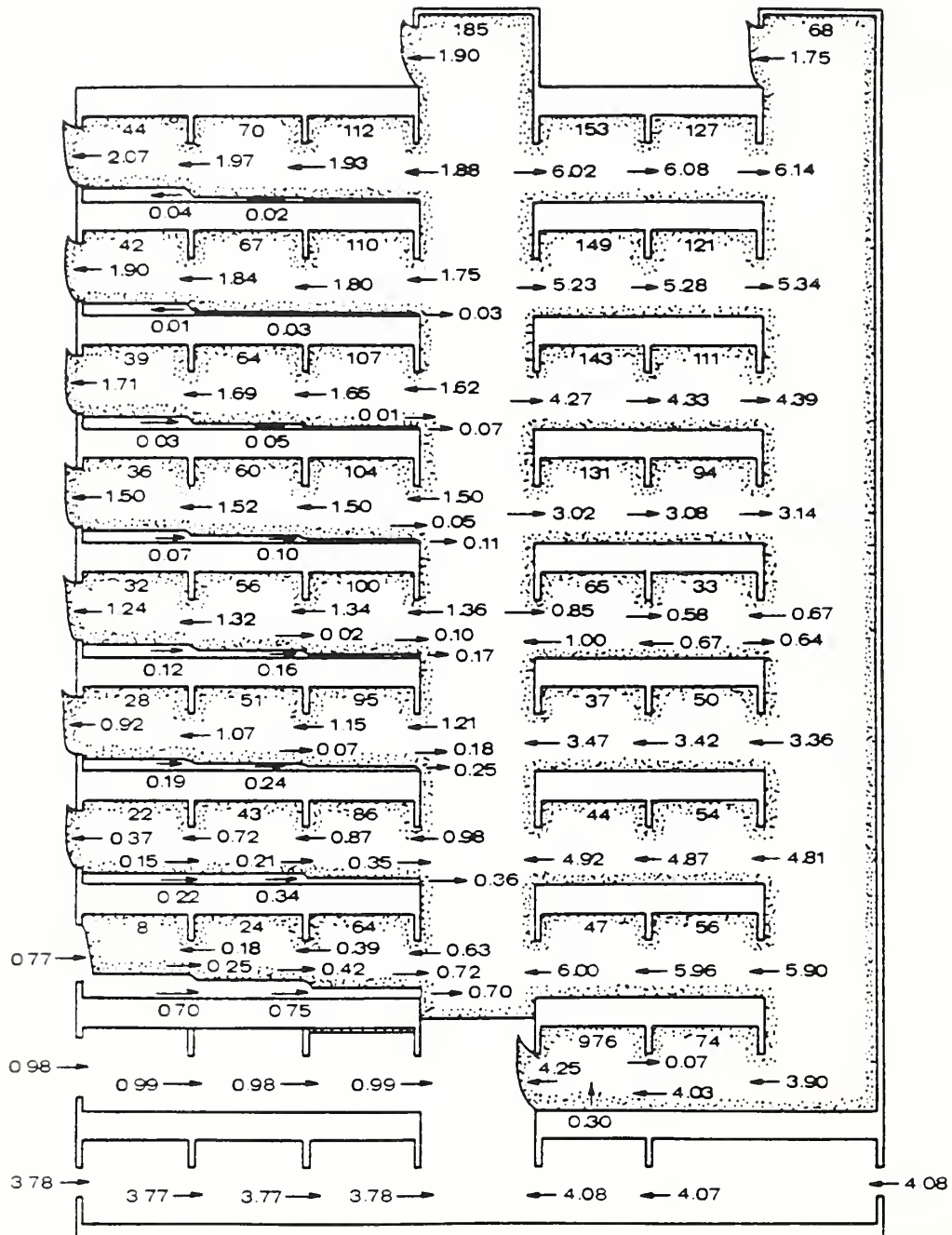
Note: Number under a ceiling with no arrow indicates temperature rise above ambient ($^{\circ}\text{C}$), and number at an opening with an arrow indicates flow rate (kg/s). (A temperature rise of 1°C = a rise of 1.8°F , and $1\text{ kg/s} = 132\text{ lb/min.}$)

Figure 14. Smoke flow at 0.5 minutes after ignition in a ten story building calculated by a zone model [Adapted from Tanaka (1983)]



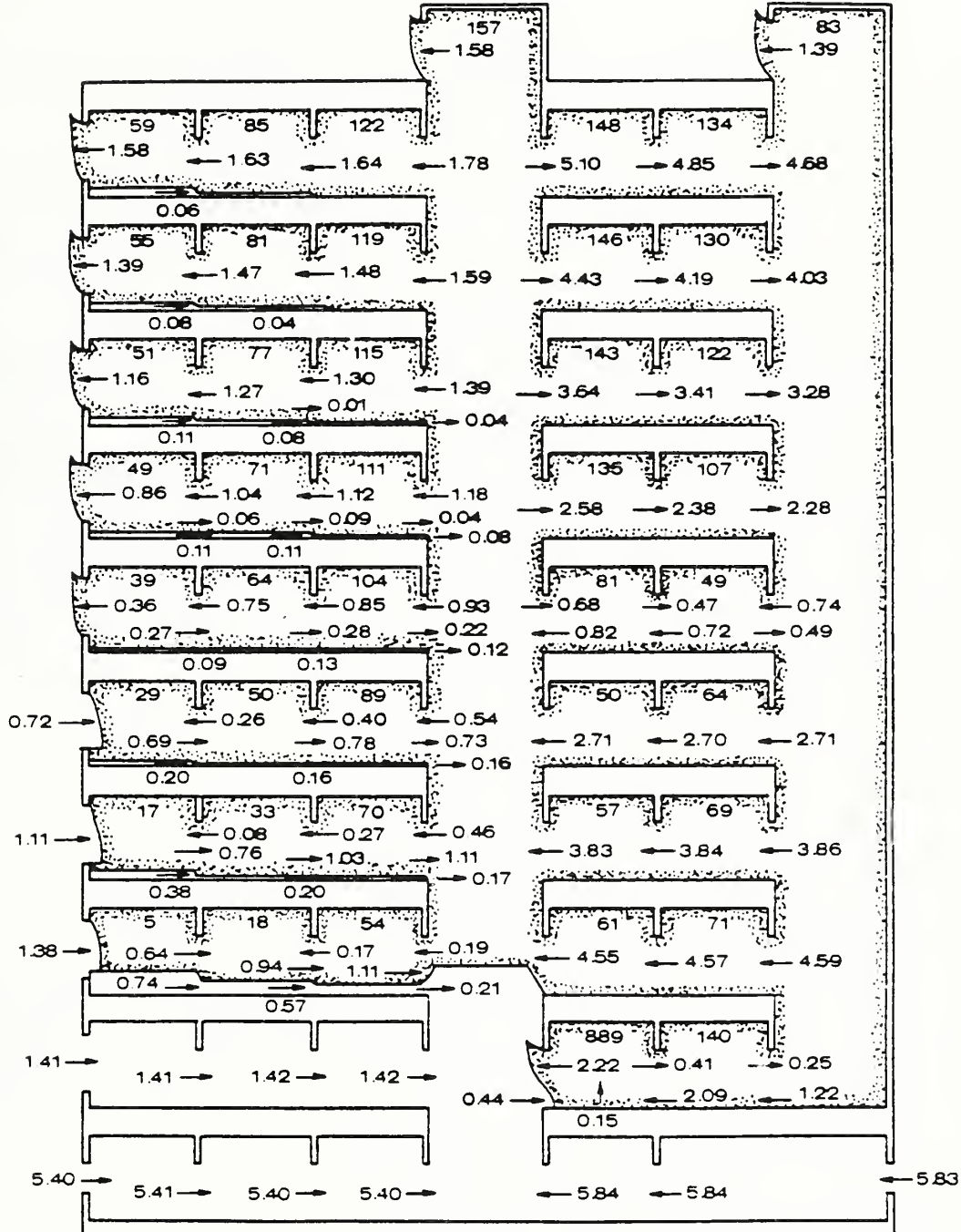
Note: Number under a ceiling with no arrow indicates temperature rise above ambient ($^{\circ}\text{C}$), and number at an opening with an arrow indicates flow rate (kg/s). (A temperature rise of 1°C = a rise of 1.8°F , and $1 \text{ kg/s} = 132 \text{ lb/min}$.)

Figure 15. Smoke flow at 1.0 minutes after ignition in a ten story building calculated by a zone model
 [Adapted from Tanaka (1983)]



Note: Number under a ceiling with no arrow indicates temperature rise above ambient ($^{\circ}\text{C}$), and number at an opening with an arrow indicates flow rate (kg/s). (A temperature rise of 1°C = a rise of 1.8°F , and $1 \text{ kg/s} = 132 \text{ lb/min.}$)

Figure 16. Smoke flow at 3.0 minutes after ignition in a ten story building calculated by a zone model
[Adapted from Tanaka (1983)]



Note: Number under a ceiling with no arrow indicates temperature rise above ambient ($^{\circ}\text{C}$), and number at an opening with an arrow indicates flow rate (kg/s). (A temperature rise of 1°C = a rise of 1.8°F , and $1\text{ kg/s} = 132\text{ lb/min.}$)

Figure 17. Smoke flow at 4.5 minutes after ignition in a ten story building calculated by a zone model [Adapted from Tanaka (1983)]

The current zone models assume instant plume rise and instant lateral smoke transport within a compartment. This omission can give rise to unrealistically quick smoke propagation in large buildings. Data from full-scale building and scale model experiments are needed to evaluate these effects fully.

At 4.5 minutes (figure 17), a fire induced stack effect has been achieved with flow from the outside into the building on the lower five floors and with flow out of the building on the upper five floors. Of course, this stack effect is due to the elevated temperatures inside most of the building. It is interesting that the flow on the bottom floor, on upper two floors, and through all exterior opening is unidirectional. In this example, the smoke spread was extensive even though both shafts were top vented. However, the vent areas for this calculation were 1.1 ft^2 ($.1 \text{ m}^2$) which is small for shaft vent opening. Network calculations discussed in the next section also show extensive smoke spread through buildings with vented shafts under conditions of normal stack effect.

It can also be seen from figure 17 that at 4.5 minutes the upper layer in most of the rooms has descended to or very near to the floor. Thus these rooms can be thought of as being almost entirely at the upper layer conditions. So for this example, the zone model predicts room conditions that almost match the perfect mixing assumption of the zone models. The treatment of shafts by these two models is very different. Zone models treat shafts as another room with upper and lower layers as illustrated in figures 14 through 17. Network models treat shafts as a vertical series of perfectly mixed spaces, one space for each floor as are illustrated in examples in the next section. Intuitively it seems that the zone approach might be more appropriate for straight open shafts such as elevator shafts, and that the network approach might be more appropriate for shafts where rising flow is accompanied by many changes in direction such as with stairwells. However, smoke could behave differently from either approach, and research is needed in this area.

8. STEADY FLOW NETWORK CALCULATIONS

The inability to simulate multi-directional flow is a shortcoming of network models. Where the pressure difference due to stack effect is sufficiently large, it will dominate the fire induced pressures resulting in unidirectional flow. Generally, the pressure difference due to buoyancy is on the order of .1 in H₂O (25 Pa), and this is usually the most important fire-induced pressure. For tall buildings during times of extreme outside temperature, stack effect pressure differences can be one or two orders of magnitude greater than the buoyancy value. However, stack effect pressure differences will still approach zero near the neutral plane. When considering gross smoke flows throughout a building, some inaccuracies near the neutral plane can be accepted. Thus, network models can be used to gain some understanding of the gross smoke flow under stack effect conditions.

Table 4. Flow areas and other data about building for example analyses

Flow areas per floor:	Flow Areas	
	ft ²	(m ²)
Exterior walls	0.84	(0.078)
Between floors	0.40	(0.037)
Stairwells to building with door closed	0.20	(0.019)
Stairwells to building with a door	10.00	(0.929)
Elevator to building	1.20	(0.111)
Elevator vent at top of shaft	4.00	(0.372)
Stairwell vent an top of shaft	10.00	(0.929)
Other data:		
Exterior air temperature	0 °F	(-18 °C)
Interior air temperature (except where noted below for cases 4A and 6A)	72 °F	(22 °C)
Fire Floor (4th floor) for cases 4A and 6A	800 °F	(427 °C)
Temperature above the 3rd floor for all shafts of case 4A	350 °F	(177 °C)
Temperature above the 3rd floor for elevator shaft and west stairwell of case 6A	350 °F	(177 °C)
Flow coefficient for all flow paths	.65	
Height between floors	10.0 ft (3.05 m)	
Location of fire	fourth floor	

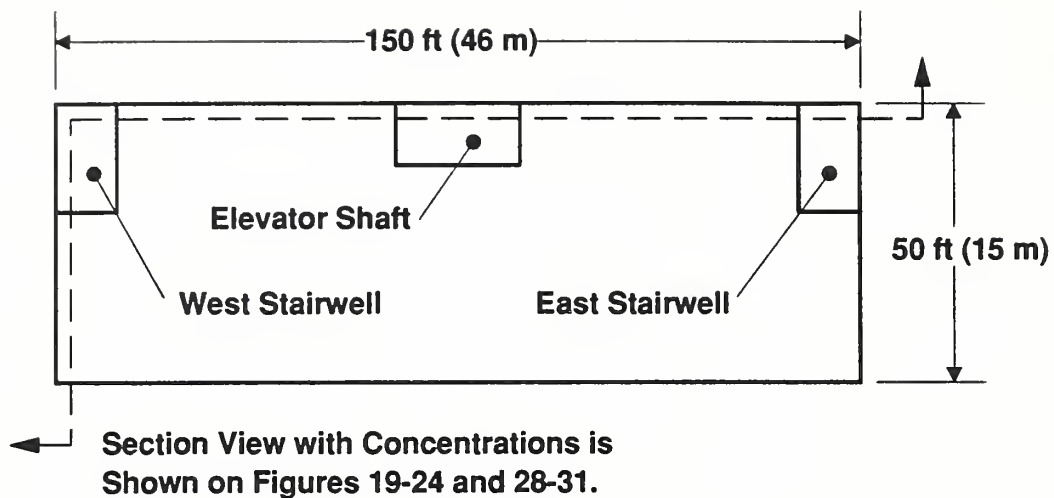


Figure 18. Floor plan of building used for example analyses

To study the effects of vents and open doors, an example building was devised and network calculations were performed for six cases. The building is twenty stories, each 50 by 150 ft (15 by 46 m) with an elevator shaft and two stairwells as shown in figure 18. The height between floors is 10.0 ft (3.05 m). The flow areas and other data for the analysis are listed in table 4. The leakage areas were selected for a building of about average tightness. The leakage areas of the walls and floors are based on data in appendix C of the ASHRAE Smoke Control Manual (Klote and Fothergill 1983). The leakage areas of the elevator walls and doors are based on data of Tamura and Shaw (1976). The following cases were analyzed for an outside temperature of 0 °F (-18 °C) and an indoor temperature of 72 °F (22 °C):

1. building without any vents or open doors,
2. building with a top vented elevator shaft,
3. building with a top vented stairwell,
4. building with a top vented elevator shaft and a top vented stairwell,

5. building with a top vented elevator shaft and a stairwell with a top vent and an open exterior, first floor door, and
6. building with a top vented elevator shaft and a stairwell with an open exterior, first floor door.

Cases 4 and 6 were recalculated with elevated shaft temperatures as cases 4A and 6A. The conditions of doors and vents for these cases are listed in table 5. For all these cases, the fire was on the fourth floor. Mass flow calculations were made with the ASCOS program (Klote and Fothergill 1983), and the resulting mass flow rates are listed in tables 6 through 11. Steady smoke concentrations relative to the fire floor concentration were calculated using these mass flow rates and equation (34). These concentrations and directions of mass flow are shown on figures 19 through 24. Steady smoke concentration analysis was employed, because this provides a basic level of understanding of some of the processes involved in this type of smoke transport. However, some questions can only be addressed by an unsteady analysis, as is discussed later.

In the following discussion of these six cases, some thought should be given as to the desired benefits of actions that could be taken to modify smoke flow. Three possible benefits are:

- Reduction in hazard conditions on the floors of a building
- Reduction in hazard conditions in a stairwells or an elevator shaft
- Reduction in smoke concentration on the fire floor

However important the last benefit might be, these analyses can not address it in that they consider the fire floor concentration constant. With

regard to the first two potential benefits, a hazard analysis of the smoke concentrations is beyond the scope of this paper.

Table 5. List of vent and door conditions for example analyses

Case	Elevator Top Vented	East Stairwell Top Vented	East Stairwell First Floor, Exterior Door Open
1	No	No	No
2	Yes	No	No
3	No	Yes	No
4	Yes	Yes	No
5	Yes	Yes	Yes
6	Yes	No	Yes
4A	Yes	Yes	No
6A	Yes	No	Yes

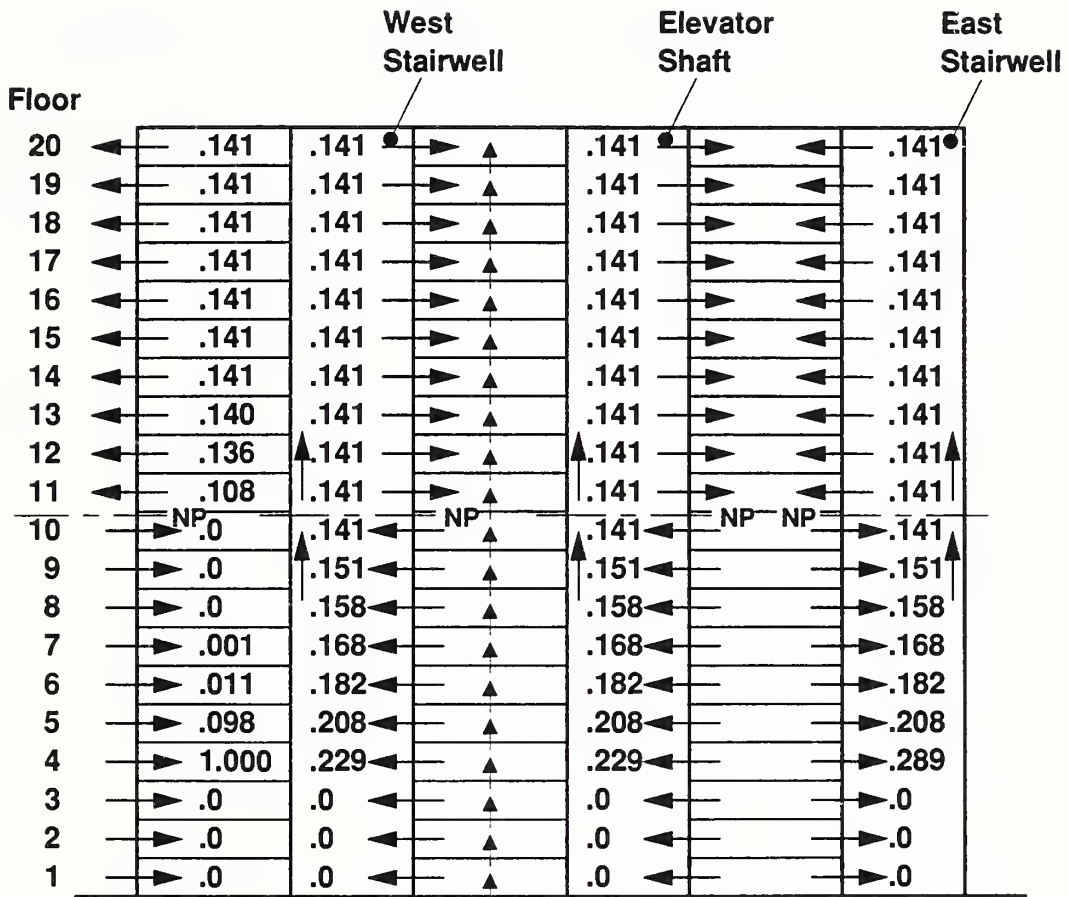
Note: All doors not addressed in the table are closed including all doors of the west stairwell. Areas of openings are listed in table 3.

8.1 Building with Doors Closed and No Vents (Case 1)

Buildings with all doors closed and without any vents are not common in the United States. However, this case was included to provide a comparison with other cases. As expected, the neutral planes for all the shafts are at the same elevation (figure 19). The concentrations below the fire floor are all zero, but this is not always so as will be shown later.

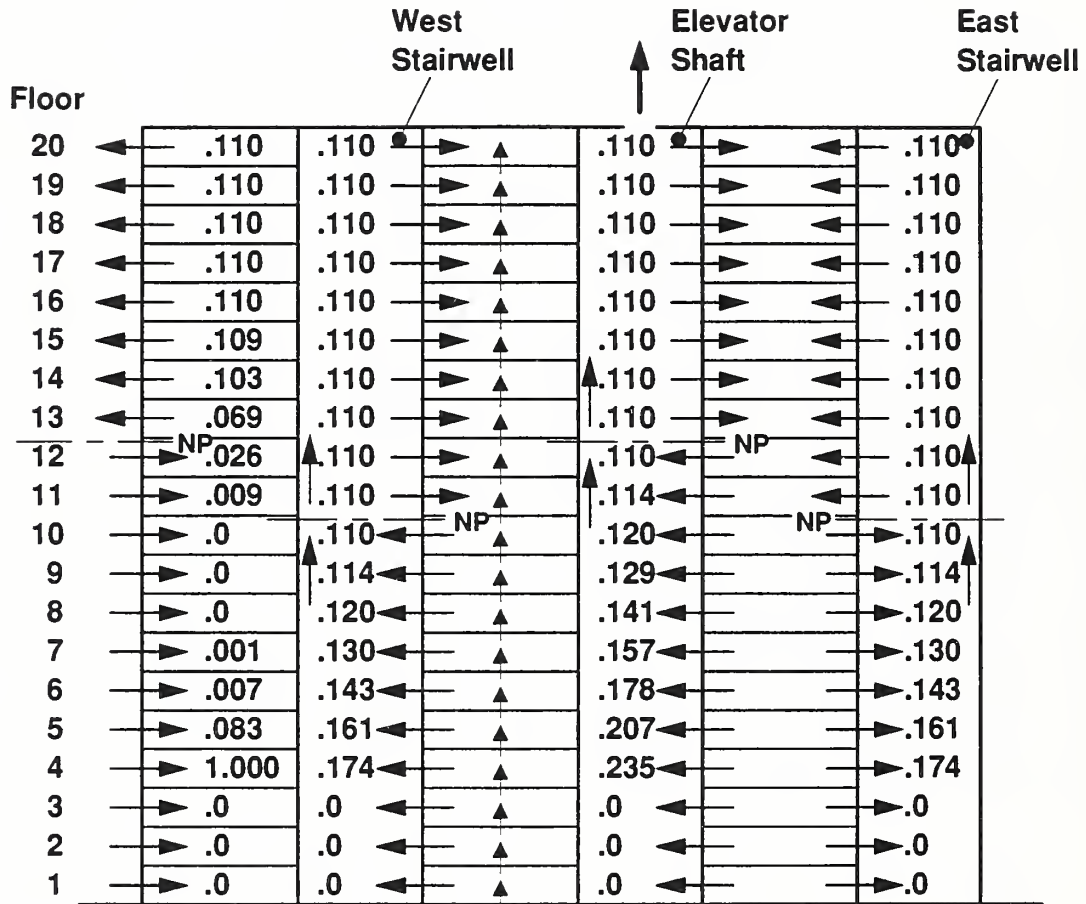
It is interesting to note that for every floor above the fire floor, the concentration decreases by about an order of magnitude up to the neutral plane². This pattern is true for all six cases analyzed. The concentrations at each level of the three shafts are the same, even though the leakage areas to the stairwells are much smaller than those to the elevator shaft. Because shaft friction is negligible, the pressures in all the three shafts are described by equation (2), $P_s = P_a - \rho_s g h$. Because the temperature is the

²Concentrations less than 0.1 % of the fire floor are not shown on figures 19 through 24.



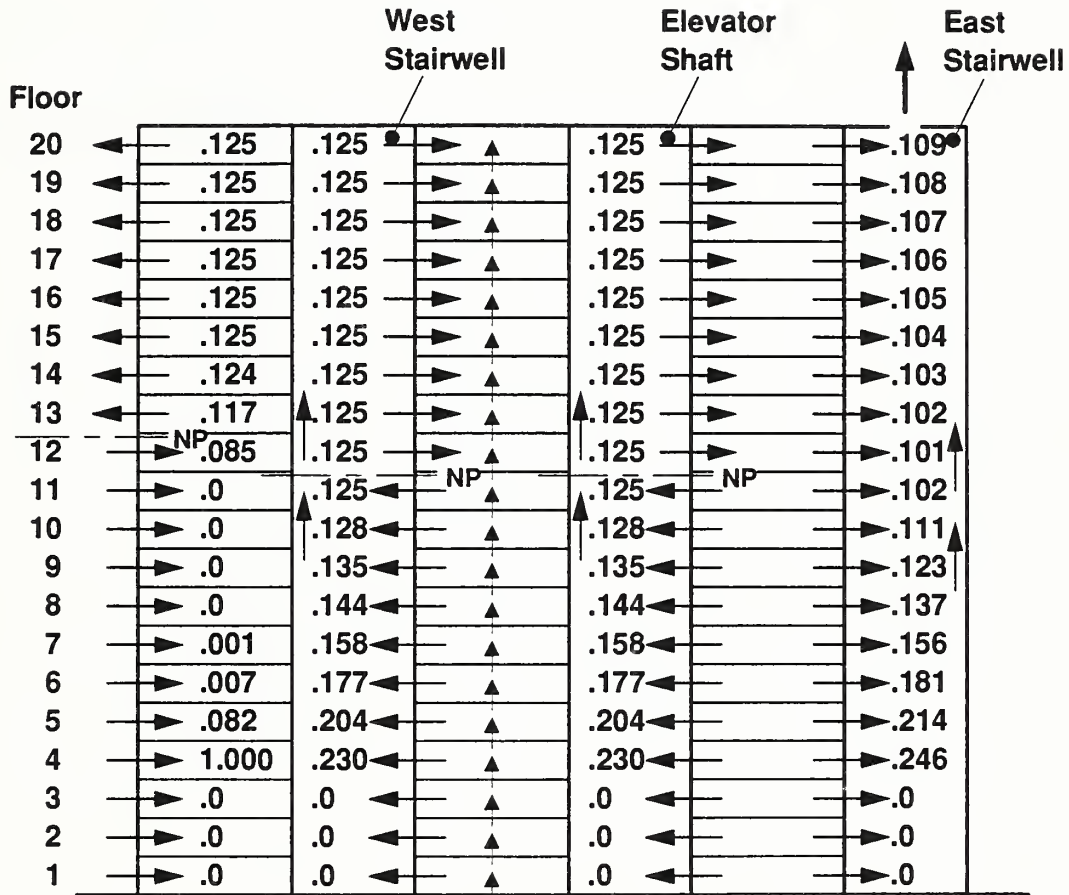
Note: Arrows indicate direction of airflow. The magnitudes of air flow rate are listed in table 6, and the flow areas data are listed in table 4. Smoke concentrations are relative to the fire floor concentration

Figure 19. Calculated smoke concentrations due to a fourth floor fire in a 20 story building without any vents or open doors (Case 1)



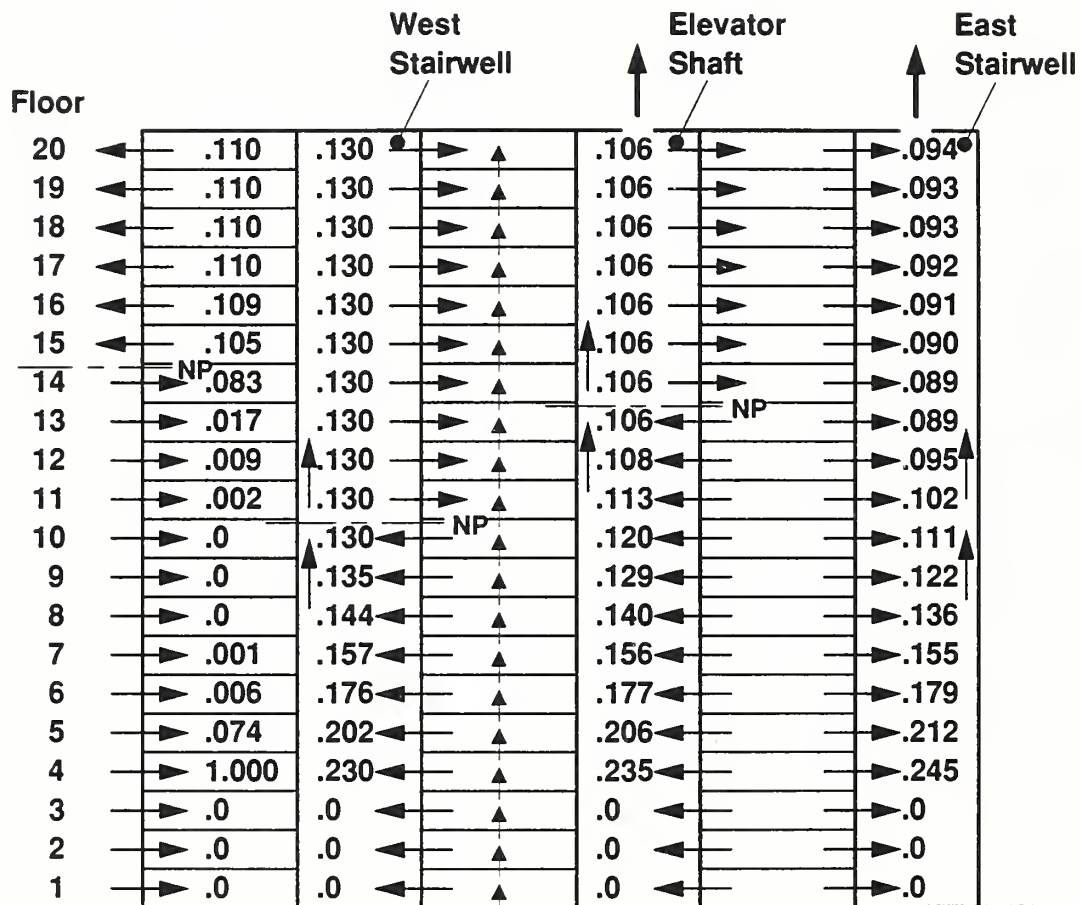
Note: Arrows indicate direction of airflow. The magnitudes of air flow rate are listed in table 7, and the flow areas data are listed in table 4. Smoke concentrations are relative to the fire floor concentration

Figure 20. Calculated smoke concentrations due to a fourth floor fire in a 20 story building with a top vented elevator shaft (Case 2)



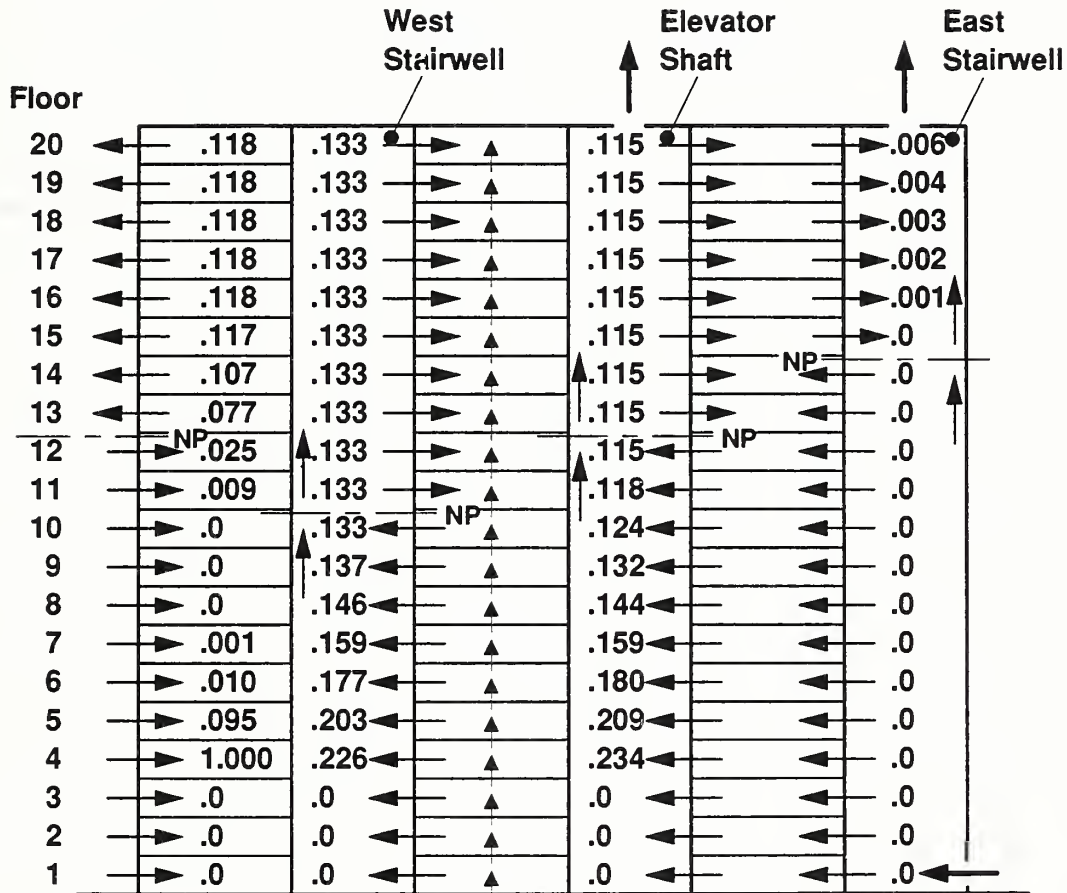
Note: Arrows indicate direction of airflow. The magnitudes of air flow rate are listed in table 8, and the flow areas data are listed in table 4. Smoke concentrations are relative to the fire floor concentration

Figure 21. Calculated smoke concentrations due to a fourth floor fire in a 20 story building with a top vented stairwell (Case 3)



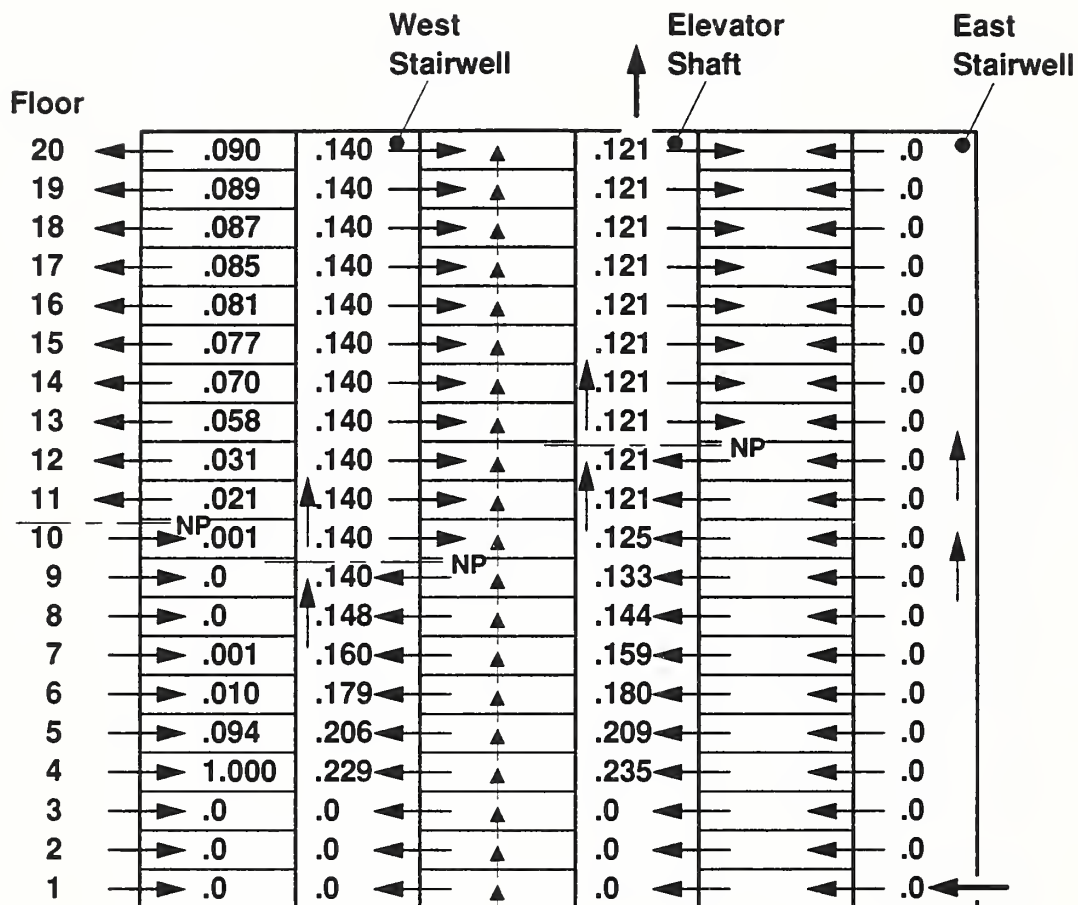
Note: Arrows indicate direction of airflow. The magnitudes of air flow rate are listed in table 9, and the flow areas data are listed in table 4. Smoke concentrations are relative to the fire floor concentration

Figure 22. Calculated smoke concentrations due to a fourth floor fire in a 20 story building with top vents in elevator and stair shafts (Case 4)



Note: Arrows indicate direction of airflow. The magnitudes of air flow rate are listed in table 10, and the flow areas data are listed in table 4. Smoke concentrations are relative to the fire floor concentration

Figure 23. Calculated smoke concentrations due to a fourth floor fire in a 20 story with top vents in elevator and stair shafts and an open stair door (Case 5)



Note: Arrows indicate direction of airflow. The magnitudes of air flow rate are listed in table 11, and the flow areas data are listed in table 4. Smoke concentrations are relative to the fire floor concentration

Figure 24. Calculated smoke concentrations due to a fourth floor fire in a 20 story building with top vents in elevator and stairwell shafts and with an open stairwell door (Case 6)

same for all three shafts, the shaft pressures are the same, and the pressure differences between the shafts and the building are the same. Thus the flows into or out of the shafts are directly proportional to one another. From this it is apparent that shaft concentrations calculated by equation (34) would be equal to one another.

Above the neutral plane the shaft concentrations do not change with height. All the mass entering a one floor height level of a shaft is from the level directly below, and it is at the concentration of that lower level. Because there is no other flow into the space to dilute the smoke, its concentration is the same as the lower level. Above the neutral plane, smoke from the shafts flows into the building spaces resulting in the considerable smoke concentration of about 14% of the fire floor concentration.

The flows from one floor to another are upward (figure 19) as might be expected during conditions of normal stack effect. For all of the examples where the building is at one temperature, the flow between floors (from one floor to another) is upward as can be observed from figure 19 to 24.

8.2 Top Vented Elevator Shaft (Case 2)

Venting the elevator shafts results in different locations of neutral plane for the elevator shaft, the stairs shafts, and between the building and the outside (figure 20). As expected, the neutral plane of the elevator shaft is higher when vented (from floor 10 to floor 13). Smoke vents out of this top vent, and the resulting concentrations on the upper floors is reduced from 14% to 11% of the fire floor. This reduction should not be considered a significant benefit. Even though smoke is vented out of the building by the elevator shaft, the other shafts carry significant quantities of smoke to the upper floors.

8.3 Top Vented Stair Shaft (Case 3)

The flow areas (table 4) of the vented stairwell differ from those of the vented elevator shaft (case 2) in that the stairwell doors are much less leaky and the vent area at the top of stairwell is much larger. These different areas result in flows that differ from those of case 2 in two significant ways. First, there is no neutral plane between the building and the vented stairwell (Figure 21). Second, the concentrations on the upper floors is higher for the vented stairwell at 12.5% of the fire floor as opposed to 11%. There is a neutral plane between the vented stair and the outside as illustrated in figure 25. The stair vent at 10 ft² (0.929 m²) is relatively large, accordingly the neutral plane to the outside is near the top of the shaft. This results in an under-pressure of the stair with respect to the building.

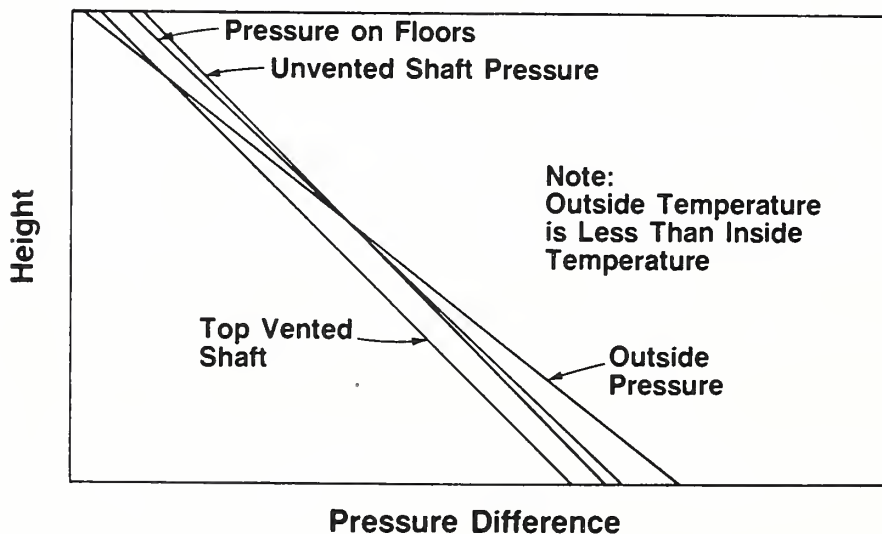


Figure 25. Pressures for a building with a top vented shaft

Intuitively, it seems from figure 25, that if the stair had been bottom vented, it would be pressurized with respect to the building. This is so as is discussed for case 6 below. Also, it can be seen on figure 25 that the slope of the pressure curve is the same as that for the unvented shaft. This is because both are at the same temperature and shaft friction is negligible.

It might be thought that a shaft with such an under-pressure would be effective at venting smoke from the building. However, the leakage around the stairwell doors are much less than that around the elevator doors, thus less smoke is vented by the vented stairwell.

8.4 Top Vents on Stair and Elevator Shafts (Case 4)

Venting the stairwell in the building with a vented elevator results in no significant change in smoke concentrations on the floors or in the shafts as shown in figures 20 and 22.

8.5 Top and Bottom Vented Stair Shaft (Case 5)

Venting both the top and bottom of a stair results in considerable flow through that stair shaft, 587 lb/min (4.44 kg/s) out the top as opposed to 264 lb/min (2.00 kg/s) with the bottom vent closed (tables 9 and 10). This large flow results in significant friction loss in the shaft, thus the slope of the pressure curve is different for this shaft from the unvented shaft as is illustrated in figure 26.

Comparisons of top and bottom venting (figure 23) with top venting (figures 20, 21 and 22) shows that top venting does not result in any significant improvement in concentrations on the floors. However, the concentrations in the vented stairwell are zero up to the fourteenth floor. This is significant, but the potential for improvement of bottom venting by itself is greater as discussed below.

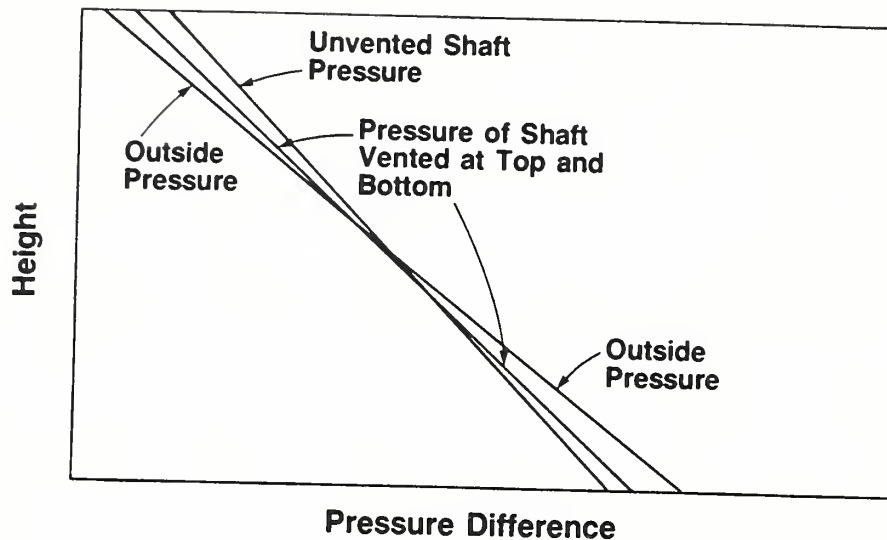


Figure 26. Pressures for a building with a shaft vented at the top and bottom

8.6 Bottom Vented Stair Shaft (Case 6)

Venting the stairwell at the bottom results in a stairwell that is pressurized with respect to the rest of the building. The concentrations in the bottom vented stair are zero as shown on figure 24. This shaft pressurization by bottom venting could have benefits for fire fighters and building occupants. There is no neutral plane between the vented shaft and the building, but there is a neutral plane between the vented stair shaft and the outside near the bottom of the building as shown on figure 27. Friction losses are slight for these shafts, and so the slopes of the vented and unvented shafts are nearly the same.

Comparisons of bottom venting (figure 24) with all the other cases (figures 19 through 23) shows that bottom venting does not result in any significant improvement in concentrations on the floors, but it results in significant improvement in the vented shaft. Bottom venting pressurizes the shaft with respect to the rest of the building, and the concentrations in the

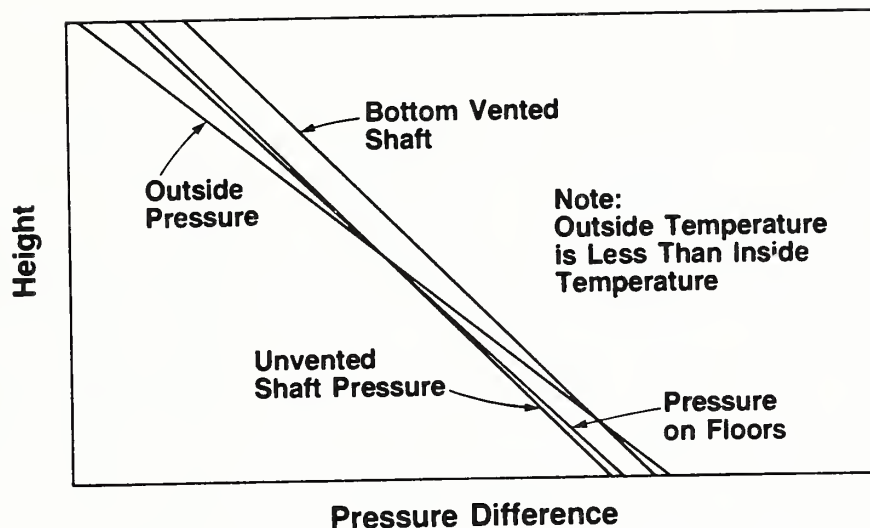


Figure 27. Pressures for a building with a bottom vented shaft

bottom vented stairwell are zero at all levels. However, this analysis does not include the effects of elevated temperatures which are addressed below.

8.7 Effect of Elevated Temperatures (Cases 4A and 6A)

To examine the effects of buoyancy of combustion gases two examples were calculated with elevated temperatures of smoke contaminated spaces. Temperatures of 350 °F (177 °C) in smoke contaminated portions of the shafts and 800 °F (427 °C) on the fire floor were arbitrarily selected. Figure 28 shows the calculated smoke concentrations due to a fourth floor fire in a 20 story building with top vents in elevator and stairwell shafts and with elevated shaft temperatures (Case 4A). The elevated temperatures resulted in a downward flow between floors except for the fire floor and the floor above. The hot gases in the shaft and the relatively cooler gases in the building can be thought of as acting like reverse stack effect in an air conditioned building when it is hot outside. This 'reverse stack effect' was overpowered

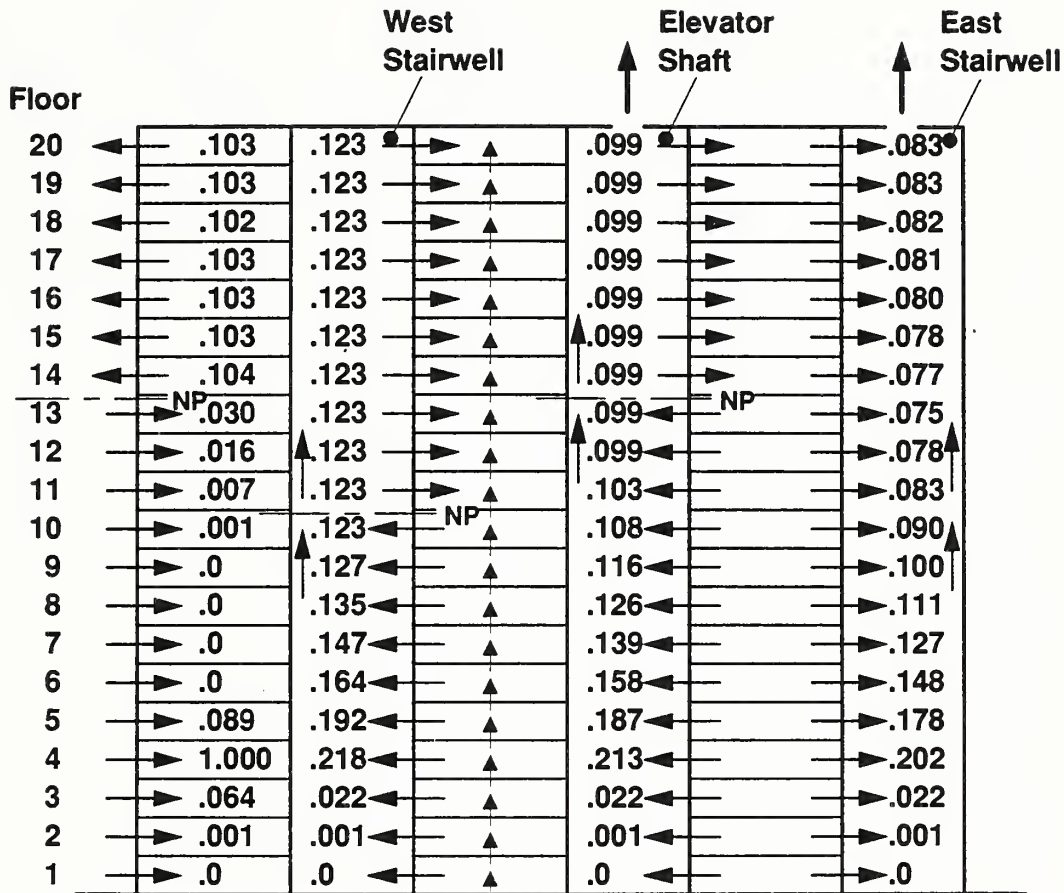
by the upward buoyancy forces on the fire floor. The downward flow resulted in smoke movement to floors below the fire floor.

Comparison of figures 22 and 28 (cases 3 and 3A) shows that the concentrations are slightly lower with elevated temperatures, but this concentration reduction is believed to be insignificant. It can also be observed from these two figures that the location of the neutral plane are almost the same for both cases. This is because the location of a neutral plane is a weak function of temperature and a strong function of leakage areas.

Figure 29 shows calculated smoke concentrations due to a fourth floor fire in a 20 story building with a top vented elevator, with an open stairwell door, and with elevated shaft temperatures (Case 6A). As with case 6 (figure 24), this shows that bottom venting of a shaft can pressurize the shaft with respect to the building. A weakness of this analysis is that the network model does not allow bidirectional flow at openings. If fire induced pressures are large enough, they can overcome the stack effect pressurization causing smoke infiltration into the stair shaft. For this example the pressure difference from the shaft to the building at the fire floor is 0.13 in H_2O (32 Pa). From the preceding discussion of buoyancy of combustion gases, a fully involved fire in a spaces of normal floor-to-ceiling height [8 to 10 ft (2.4 to 3 m)] will result in a buoyancy pressure difference of about 0.06 in H_2O (15 Pa). This buoyancy force is insufficient to overcome the stack effect pressurization of this example. If the fire were on a higher floor, shaft pressurization would have still prevented smoke infiltration to the stair because this stack effect pressurization increases with height. For example, at floor fifteen the pressurization is .19 in H_2O (47 Pa).

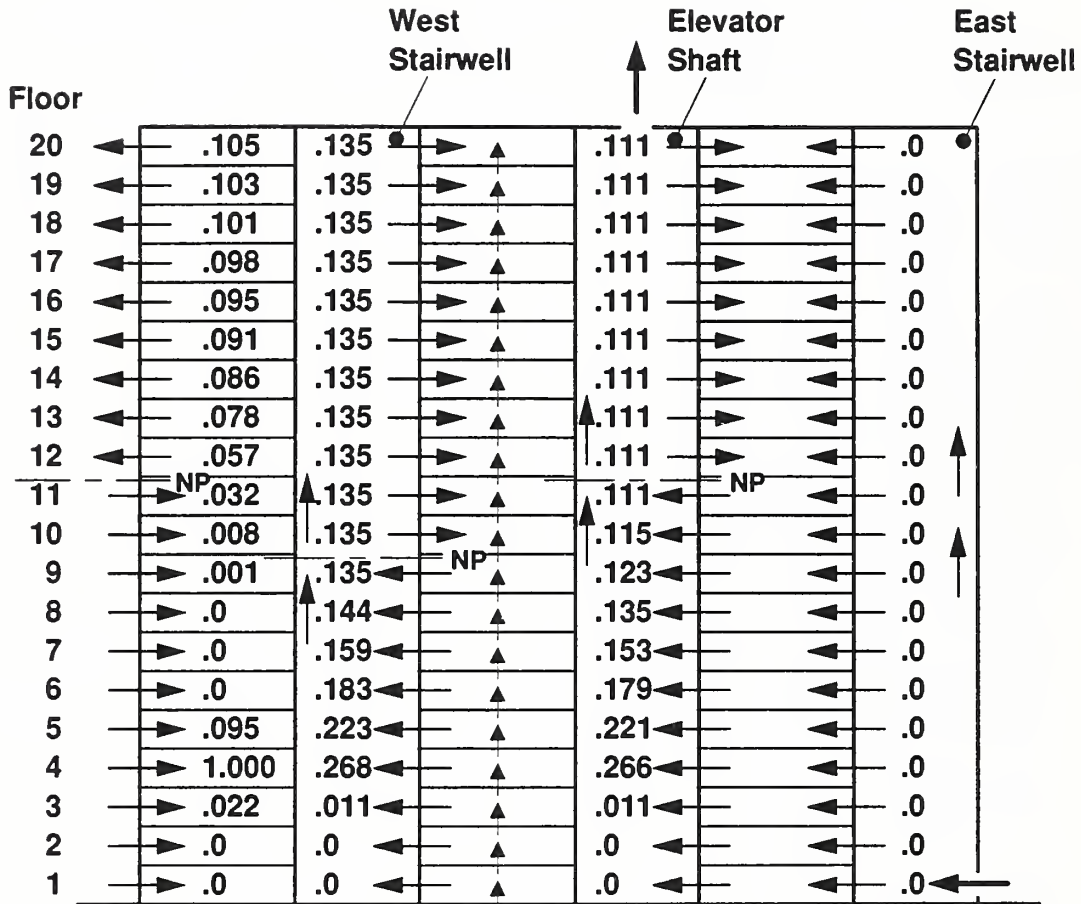
8.8 Fire Above the Neutral Planes

Above the neutral plane between a shaft and the building, the forces of normal stack effect pressurize the shaft with respect to the building space. If this pressurization is large enough relative to fire induced pressure differences, smoke will not enter the shaft. Figure 30 shows the steady



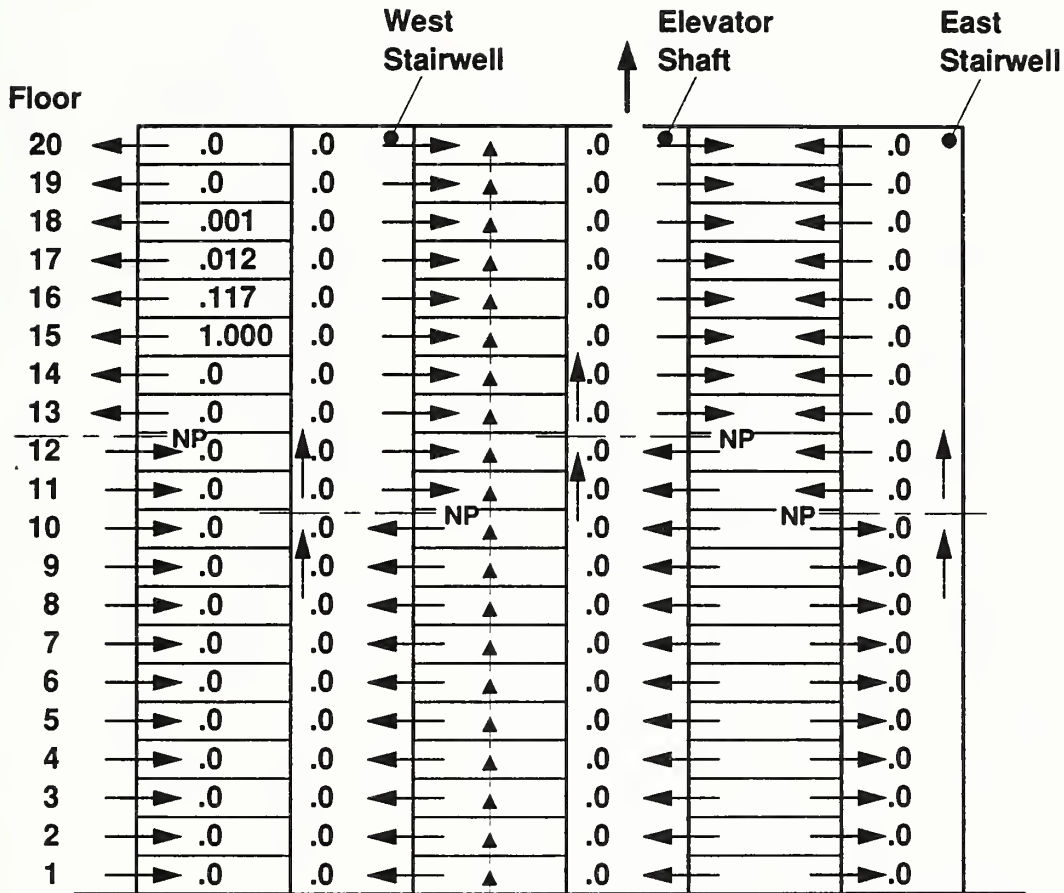
Note: Arrows indicate direction of airflow. The magnitudes of air flow rate are listed in table 12, and the flow areas data are listed in table 4. Smoke concentrations are relative to the fire floor concentration

Figure 28. Calculated smoke concentrations due to a fourth floor fire in a 20 story building with top vents in elevator and stairwell shafts and with elevated shaft temperatures (Case 4A)



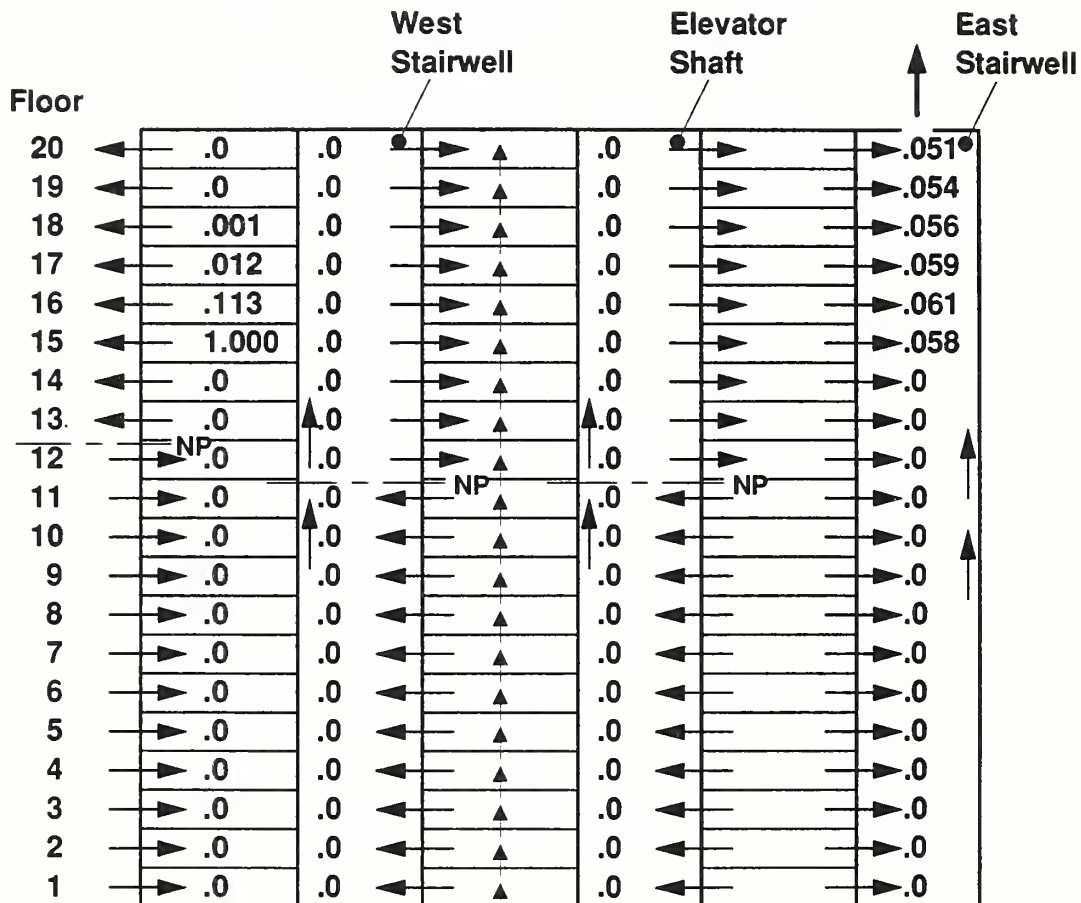
Note: Arrows indicate direction of airflow. The magnitudes of air flow rate are listed in table 13, and the flow areas data are listed in table 4. Smoke concentrations are relative to the fire floor concentration

Figure 29. Calculated smoke concentrations due to a fourth floor fire in a 20 story building with a top vented elevator, with an open stairwell door, and with elevated shaft temperatures (Case 6A)



Note: Arrows indicate direction of airflow. The magnitudes of air flow rate are listed in table 7, and the flow areas data are listed in table 4. Smoke concentrations are relative to the fire floor concentration

Figure 30. Calculated smoke concentrations due to a fifteenth floor fire in a 20 story building with a top vented elevator shaft (Modification of case 2)



Note: Arrows indicate direction of airflow. The magnitudes of air flow rate are listed in table 8, and the flow areas data are listed in table 4. Smoke concentrations are relative to the fire floor concentration

Figure 31. Calculated smoke concentrations due to a fifteenth floor fire in a 20 story building with a top vented stairwell (Modification of case 3)

concentrations calculated for a fifteenth floor fire in a building with a top vented elevator shaft (mass flow rates from case 2). The figure shows no smoke contamination of the shafts, but the pressure differences are not sufficient to prevent smoke infiltration into the shafts from a fully developed fire. At the fifteenth floor, the pressure differences are 0.024 in H_2O (6 Pa) at the stairwells and .008 in H_2O at the elevator shaft. Obviously, the shaft pressurization by stack effect is insufficient to overcome the buoyancy forces due to a fully involved fire on a floor of normal floor-to-ceiling height. However, this shaft pressurization is sufficient to overcome smoke with little buoyancy such as from a sprinklered fire or a smoldering fire.

If the building of the example were taller and the fire floor located further above the neutral plane, stack effect pressurization would be larger. Because pressure difference is nearly a linear function of height, the pressure differences at floor fifteen can be extrapolated to approximate that at other floors. At 28 floors above the neutral plane, stack effect pressurization of the elevator shaft would be about .1 in H_2O (25 Pa) which would prevent smoke infiltration due to buoyancy. Considering that the neutral plane is roughly at the building mid-height, this method of limiting smoke flow for fully developed fires can only work for very tall buildings.

To examine the effect of stair shaft venting, calculations of steady concentrations were made a fifteenth floor fire in a building with a top vented stairwell (mass flow rates from case 3). The smoke concentrations (figure 31) on the floors above the fire floor for this case are almost the same as without stairwell venting (figure 30). However, stairwell venting does result in smoke in the stairwell which is a serious drawback. For this example, there is no apparent advantage of stairwell venting.

9. FUTURE EFFORT

While some aspects of smoke transport due to stack effect can be analyzed adequately, no existing model is capable of dealing with the total

problem. Of course, the capability of unsteady analysis is most important, and the ability to simulate multi-directional flow between compartments is also needed. Any model intended to deal with this problem must incorporate pressure changes with elevation in a consistent manner over the entire building and the outdoors. Also incorporation of wind effects is desired.

It is planned to extend a zone model, to develop a tool appropriate for analysis of smoke flow in large buildings. An important part of such a model is a specific submodel for smoke transport in shafts. Such a submodel needs to incorporate shaft friction, because such friction pressure losses can be significant in many common situations. Because of the vast differences between stairwells and most other shafts, it seems that two different types of shaft submodel may be needed. Even though smoke transport under conditions of reverse stack effect have not been addressed in this paper, this topic is of sufficient concern that shaft submodels should be capable of simulating it. This extended zone model will be used study smoke transport under a variety of conditions including shaft venting, fan pressurization for smoke control, and fire reconstruction.

Experimental studies are needed to guide and evaluate the development of the computer model discussed above, and a series of full scale and scale model experiments are planned.

9.1 Full Scale Experiments

Full scale smoke control and smoke transport experiments will be conducted in 1989 at the seven story Plaza Hotel Building in Washington DC (Klote 1988b). Smoke control will be achieved by exhausting the fire zone and pressurizing surrounding zones, and by pressurizing stairwells. The smoke control systems were designed using the analysis methods in the NBS Smoke Control Handbook and the design pressures recommended in NFPA 92A. The effectiveness of these systems to limit smoke flow will be measured, and the interaction between smoke control and fire development will be studied. Experiments without smoke control will be used to study smoke flow under stack effect conditions.

9.2 Scale Model Experiments

Scale model experiments in a seven story building including the stairwell, elevator shaft, and a forced air heating and cooling system will be conducted under "winter" and "summer" stack effect conditions. Several of the walls of the model will be of glass to allowing video recordings to be made of the smoke flow up the stairwell and elevator shafts. Adjustable openings in walls and floors will simulate the building leakage paths to allow simulation of various building leakage areas and open and closed doors. It is anticipated that Plaza Hotel experiments and the scale model experiments will provide an understanding of the mechanisms involved in such smoke flow, and that this understanding will be the basis of a mathematical model.

10. CONCLUSIONS

1. Operation of elevators by the fire service during a fire can result in smoke being pulled into the elevator shaft by piston effect. It seems a safe recommendation that fire fighters should favor the use of elevators in multiple car shafts over ones in single car shafts to reduce the likelihood of smoke being pulled into the elevator shaft as a result of elevator car motion.
2. Location of the neutral plane is a strong function of flow areas and a weak function of temperature. Thus different venting conditions have a major effect on the locations of the neutral plane, while different temperatures have a very slight effect on the location of the neutral plane.
3. Regardless of whether a vent in a shaft is above or below the neutral plane, the neutral plane between the shaft and the outside will be located between the height described by equation (23) for an unvented shaft and the vent elevation, H_v . Further, the smaller the value of $A'H/A_v$, the closer the neutral plane will be to H_v .

4. While pressure losses due to friction generally are negligible for shafts with all doors closed and no vents, shaft friction can be significant for many common situations such as a shaft with an open door or a vent.
5. For the example network analyses presented in this paper, venting shafts at the top, bottom or at both top and bottom does not result in any significant reduction in smoke concentrations on the floors of the building.
6. As shown in the example network analyses for low outside temperatures, bottom venting of a shaft can result in a pressurization of that shaft that can prevent smoke infiltration into it. This bottom venting can be accomplished by opening an exterior stairwell door. The magnitude of this shaft pressurization increases with height.
7. As demonstrated by example network analysis, elevated temperatures of combustion gases can result in downward smoke flows between floors of a building.
8. For fires above the neutral plane, as shown by the example calculations, normal stack effect tends to pressurize shafts and limit smoke flow to the fire floors and to a number of floors above the fire floor. This happens even without shaft venting. However, this shaft pressurization can be overpowered by fire induced forces such as buoyancy of combustion gases. For fully developed fires, the example case analyzed indicated that this approach is only appropriate for buildings taller than about 60 stories.
9. Further research consisting of computer modeling coupled with a program of experimentation is needed in order to develop the capability to analyze smoke transport in large buildings under the conditions of stack effect, open stairwell doors and vents that commonly happen during building fires.

11. ACKNOWLEDGMENTS

Many people have given valuable advice and suggestions during this project. In particular, the author thanks Chief Elmer Chapman formerly of the New York City Fire Department, Leonard Cooper of the National Institute of Standards and Technology, Robert Fitzgerald of Worcester Polytechnic Institute, James Quintiere of the National Institute of Standards and Technology, Tom Smith of the US Fire Administration, and George Tamura of the National Research Council of Canada.

12. NOMENCLATURE

A	area
A'	area of continuous opening per unit height
C	flow coefficient
c	concentration of a product of combustion
b	$= \frac{g P_{atm}}{R} \left(\frac{1}{T_o} - \frac{1}{T_s} \right)$
C _s	shaft flow coefficient
D _e	effective diameter of a duct or shaft
f	friction factor of duct or shaft
g	acceleration of gravity
H	height
h	height above neutral plane
L	length of duct or height of one floor of a shaft
M	product of combustion flow rate or mass of gas above elevator car
m	mass flow rate
N	number of floors
n	wind exponent
P	absolute pressure
P _{atm}	absolute atmospheric pressure
Q _{atm}	volumetric flow rate
q	enthalpy flow rate
R	gas constant
T	absolute temperature
t	time
U	velocity
V	volume
y	average roof height
z	elevation
ρ	density
ΔP	pressure difference

ΔP_f pressure loss due to friction in duct or shaft

Subscripts

a above the neutral plane or elevator car
b below the neutral plane or elevator car
c elevator car
e effective
f fire
i building
in in
L lower layer
l lobby
o outside (or for wind at reference elevation, z_o)
out out
s shaft
U upper layer
u upper limit
w wind

13. REFERENCES

ASHRAE Handbook - 1985 Fundamentals, Chapter 22 Ventilation and Infiltration, American Society of Heating, Refrigerating and Air-Conditioning Engineers, Atlanta, GA.

Barrett, R.E. and Locklin, D.W. 1969. A Computer Technique for Predicting Smoke Movement in Tall Buildings, Symposium on Movement of Smoke on Escape Routes in Buildings, Watford College of Technology, Watford, Herts, U.K., pp. 78-87.

Butcher, E.G., Fardell, P.J. and Jackman, P.J. 1969. Prediction of the behavior of smoke in a building using a computer, Symposium on Movement of Smoke in Escape Routes in Buildings, pp. 70-75, Watford, Herts, England: Watford College of Technology.

Cooper, L.Y. 1982. A Mathematical Model for Estimating the Available Safe Egress Time in Fires, Fire and Materials, Vol. 6, Nos. 3 and 4, pp. 135-144.

Cooper, L.Y. 1984. Smoke Movement in Rooms of Fire Involvement and Adjacent Spaces, Fire Safety Journal, Vol. 77, pp. 33-46.

Cooper, L.Y. and Forney, G.P. 1987. Fire in a Room with a Hole: A Prototype Application of the Consolidated Compartment Fire Model (CCFM) Computer Code, Presented at the 1987 Combined Meetings of Eastern Section of Combustion Institute and NBS Annual Conference on Fire Research, appears in Meeting Proceedings, Combustion Institute, Pittsburgh, PA.

- Evers, E. and Waterhouse, A. 1978. A Computer Model for Analyzing Smoke Movement in Buildings, Building Research Est., Borehamwood, Herts, U.K.
- Feustel, H.E. and Kendon, V.M. 1985. Infiltration Models for Multicellular Structures - A Literature Review, Energy and Buildings, Vol. 8, pp 123-136.
- Houghton, E.L. and Carruthers, N.B. 1976. Wind Forces on Buildings and Structures: an Introduction, Wiley, New York, NY.
- Jones, W.W. 1983. A Review of Compartment Fire Models, NBSIR 83-2684, National Bureau of Standards, Gaithersburg, MD.
- Jones, W.W. 1985. Future Directions for Modeling the Spread of Fire, Smoke, and Toxic Gases, Fire safety: Science and Engineering, ASTM STP 882, T.Z. Harmathy, Ed., American Society for Testing and Materials, Philadelphia, PA, pp. 70-96.
- Kennedy, L.A. and Cooper, L.Y. 1987. Before the Smoke Clears - Heat and Mass Transfer in Fires and Controlled Combustion, Mechanical Engineering, Vol. 109, No. 4; pp. 62-67.
- Kolousek, V., Pirner M., Fischer, O. and Naprstek, J. 1984. Wind Effects on Civil Engineering Structures, Elsevier, New York NY.
- Klote, J.H. 1982. A Computer Program for Analysis of Smoke Control Systems, NBSIR 82-2512, National Bureau of Standards, Gaithersburg, MD.
- Klote, J.H. 1987. A Computer Model of Smoke Movement by Air Conditioning Systems (SMACS), NBSIR 87-3657, National Bureau of Standards, Gaithersburg, MD.
- Klote, J.H. 1988a. An Analysis of the Influence of Piston Effect on Elevator Smoke Control, NBSIR 88-3751, National Bureau of Standards, Gaithersburg, MD.
- Klote, J.H. 1988b. Project Plan of Full Scale Smoke Control and Smoke Movement Tests, NBSIR 88-3600, National Bureau of Standards, Gaithersburg, MD.
- Klote, J.H. and Cooper, L.Y. 1988. Model of a Fan-Resistance Ventilation System and its Application to Fire Modeling, to be published as NISTIR, National Institute of Standards and Technology (formerly National Bureau of Standards), Gaithersburg, MD.
- Klote, J.H. and Fothergill, J.W. 1983. Design of Smoke Control Systems for Buildings, American Society of Heating, Refrigerating and Air-conditioning Engineers, Atlanta, GA.
- Klote, J.H. and Tamura, G.T. 1986. Elevator Piston Effect and the Smoke Problem, Fire Safety Journal, Vol 11 No 3, pp 227-233.
- Klote, J.H. and Tamura, G.T. 1987. Experiments of Piston Effect on Elevator Smoke Control, ASHRAE Transactions, Vol 93, Part 2a, pp 2217-2228.

- MacDonald, A.J. 1975. Wind Loading on Buildings, Wiley, New York NY.
- McGuire, J.H. and Tamura G.T 1975. Simple Analysis of Smoke-Flow Problems in High Buildings, Fire Technology, Vol 11, No 1, pp 15-22.
- Mitler, H.E. 1985. Comparison of Several Compartment Fire Models: An Interim Report, NBSIR 85-3233, National Bureau of Standards, Gaithersburg, MD.
- Mitler, H.E. and Emmons, H.W. 1981. Documentation for CFC V, the Fifth Harvard Computer Fire Code, Home Fire Project Tech. Rep. #45, Harvard University, Cambridge, MA.
- NFPA 1988. Recommended Practice for Smoke Control Systems, NFPA 92A, Quincy, MA, National Fire Protection Assn.
- Sachs, P. 1978. Wind Forces in Engineering, 2nd Ed., Pergamon Press, New York.
- Said, M.N.A. 1988. A Review of Smoke Control Models, ASHRAE Journal, Vol 30, No 4, pp 36-40.
- Sander, D.M. 1974. FORTRAN IV Program to Calculate Air Infiltration in Buildings, National Research Council Canada, DBR Computer Program No. 37.
- Sander, D.M. and Tamura, G.T. 1973. FORTRAN IV Program to Stimulate Air Movement in Multi-Story Buildings, National Research Council Canada, DBR Computer Program No. 35.
- Quintiere, J.G., Steckler, K. and McCaffrey, B. 1981. A Model to Predict the Conditions in a Room Subject to Crib Fires, First Specialists Meeting (International) of the Combustion Institute, Talence, France.
- Simiu, E. and Scanlan, R.H. 1986. Wind Effects on Structures, 2nd Ed., Wiley, New York, NY.
- Tamura, G.T. 1969. Computer Analysis of Smoke Movement in Tall Buildings, ASHRAE Transactions, Vol 75, Part II, pp 81-93.
- Tamura, G.T. and Klote, J.H. 1988. Experimental Fire Tower Studies on Adverse Pressures Caused by Stack and Wind Action: Studies on Smoke Movement and Control, ASTM International Symposium on Characterization and Toxicity of Smoke, December 5, 1988, Phoenix, AZ.
- Tamura, G.T. and Shaw, C.Y. 1976. Air Leakage Data for the Design of Elevator and Stair Shaft Pressurization Systems, ASHRAE Transactions, Vol. 82, Part 2, pp. 179-190.
- Tamura, G.T. and Wilson, A.G. 1966. Pressure Differences for a Nine-Story Building as a Result of Chimney Effect and Ventilation System Operation, ASHRAE Transactions, Vol 72, Part I, pp 180-189.

Tamura, G.T. and Wilson, A.G. 1967a. Building Pressures Caused by Chimney Action and Mechanical Ventilation, ASHRAE Transactions, Vol 73, Part II, pp

Tamura, G.T. and Wilson, A.G. 1967b. Pressure Differences Caused by Chimney Effect in Three High Buildings, ASHRAE Transactions, Vol 73, Part II, pp

Tanaka, T., A Model of Multiroom Fire Spread, NBSIR 83-2718, National Bureau of Standards, Gaithersburg, MD, 1983.

Wakamatsu, T. 1977. Calculation Methods for Predicting Smoke Movement in Buildings and Designing Smoke Control Systems, Fire Standards and Safety, ASTM STP-614, A.F. Robertson, Ed., Philadelphia, PA, American Society for Testing and Materials, pp. 168-193.

Walton, G.N. 1984. A Computer Program for Estimating Infiltration and Inter-Room Air Flows, ASHRAE Transactions, Vol. 90, Part I.

Wood, D.J and Rayes, A.M. 1981. Reliability of Algorithms for Pipe Network Analysis, Journal of Hydraulics Division, Proceedings of the American Society of Civil Engineers, Vol. 107, No. HY10, pp 1145-1161.

Yoshida, H., Shaw, C.Y. and Tamura, G.T. 1979. A FORTRAN IV program to calculate smoke concentrations in a multi-story building, Ottawa, Canada: National Research Council.

Zukoski, E.E. and Kubota, T. 1980. Two-Layer Modelling of Smoke Movement in Building Fires, Fire and Materials, Vol. 4, No. 17.

Table 6. Calculated flow rates (lb/min) in a building without any vents or open doors (Case 1)

Floor	Into West Stairwell	Into Elevator Shaft	Into East Stairwell	To Floor Above	Into Building From Outside
20	-8.02	-48.40	-8.02	-	-68.06
19	-7.82	-47.16	-7.82	3.64	-64.01
18	-7.43	-44.84	-7.43	4.88	-60.06
17	-6.95	-41.99	-6.95	5.26	-55.99
16	-6.42	-38.79	-6.42	5.37	-51.64
15	-5.83	-35.25	-5.83	5.40	-46.90
14	-5.17	-31.30	-5.17	5.41	-41.64
13	-4.42	-26.77	-4.42	5.42	-35.59
12	-3.51	-21.26	-3.51	5.43	-28.28
11	-2.26	-13.68	-2.26	5.44	-18.26
10	1.54	9.32	1.54	5.53	12.23
9	3.22	19.52	3.22	5.73	25.95
8	4.30	26.00	4.30	5.73	34.62
7	5.15	31.18	5.15	5.74	41.52
6	5.89	35.60	5.89	5.73	47.41
5	6.54	39.53	6.54	5.73	52.67
4	7.13	43.07	7.13	5.70	57.47
3	7.66	46.22	7.66	5.59	61.96
2	8.09	48.80	8.09	5.20	66.30
1	8.33	50.20	8.33	3.92	70.79

Notes:

1. For flow areas and other data see table 3.
2. 1 lb/min = .00756 kg/s

Table 7. Calculated flow rates (lb/min) in a building with a top vented elevator shaft (Case 2)

Vent Flow:		lb/min			
Flow out top vent of elevator shaft		313.23			
Floor	Into West Stairwell	Into Elevator Shaft	Into East Stairwell	To Floor Above	Into Building From Outside
20	-8.21	-39.49	-8.21	-	-59.69
19	-8.00	-37.87	-8.00	3.76	-55.06
18	-7.61	-34.88	-7.61	4.94	-50.44
17	-7.14	-31.14	-7.14	5.26	-45.51
16	-6.63	-26.75	-6.63	5.34	-40.02
15	-6.08	-21.53	-6.08	5.32	-33.61
14	-5.50	-14.83	-5.50	5.23	-25.59
13	-4.92	-0.84	-4.92	4.96	-12.90
12	-3.41	21.38	-3.41	7.15	15.40
11	-1.38	28.48	-1.38	6.29	26.95
10	2.06	32.22	2.06	5.04	35.89
9	3.40	36.13	3.40	5.46	42.75
8	4.39	39.86	4.39	5.62	48.57
7	5.22	43.34	5.22	5.68	53.74
6	5.94	46.58	5.94	5.70	58.44
5	6.58	49.62	6.58	5.70	62.80
4	7.16	52.46	7.16	5.67	66.89
3	7.68	55.04	7.68	5.55	70.80
2	8.10	57.16	8.10	5.12	74.66
1	8.32	58.29	8.32	3.80	78.71

Notes:

1. For flow areas and other data see table 3.
2. 1 lb/min = .00756 kg/s

Table 8. Calculated flow rates (lb/min) in a building with a top vented stairwell (Case 3)

Vent Flow:		lb/min			
Flow out top vent of east stairwell		291.81			
Floor	Into West Stairwell	Into Elevator Shaft	Into East Stairwell	To Floor Above	Into Building From Outside
20	-9.31	-56.13	12.36	-	-57.41
19	-9.06	-54.62	12.38	4.32	-52.77
18	-8.59	-51.81	12.56	5.77	-48.34
17	-8.01	-48.32	12.80	6.24	-43.74
16	-7.34	-44.32	13.08	6.43	-38.74
15	-6.57	-39.70	13.38	6.57	-33.09
14	-5.65	-34.17	13.71	6.75	-26.45
13	-4.43	-26.83	14.08	7.06	-17.97
12	-2.13	-13.04	14.55	7.83	2.16
11	1.28	7.62	14.71	5.05	23.78
10	2.72	16.43	14.87	4.87	33.71
9	3.72	22.54	15.06	5.16	41.14
8	4.56	27.62	15.26	5.33	47.33
7	5.29	32.06	15.48	5.43	52.76
6	5.96	36.03	15.71	5.48	57.64
5	6.56	39.65	15.94	5.52	62.14
4	7.11	42.97	16.17	5.52	66.34
3	7.61	45.95	16.40	5.42	70.33
2	8.02	48.38	16.59	5.03	74.24
1	8.23	49.67	16.70	3.74	78.33

Notes:

1. For flow areas and other data see table 3.
2. 1 lb/min = .00756 kg/s

Table 9. Calculated flow rates (lb/min) in a building with a top vented elevator shaft and a top vented stairwell (Case 4)

Vent Flows:		lb/min			
Flow out top vent of elevator shaft		285.89			
Flow out top vent of east stairwell		264.83			

Floor	Into West Stairwell	Into Elevator Shaft	Into East Stairwell	To Floor Above	Into Building From Outside
20	-9.10	-47.22	10.69	-	-50.12
19	-8.82	-45.29	10.76	4.47	-44.78
18	-8.32	-41.75	11.01	5.88	-39.53
17	-7.70	-37.20	11.33	6.33	-33.83
16	-6.97	-31.60	11.68	6.57	-27.19
15	-6.07	-24.05	12.08	6.85	-18.69
14	-4.80	-8.88	12.56	7.47	0.72
13	-3.92	14.21	12.80	5.61	23.04
12	-2.76	22.02	13.04	5.63	32.56
11	-0.78	27.23	13.26	5.36	40.06
10	2.35	31.10	13.46	5.03	46.56
9	3.54	35.01	13.69	5.37	52.08
8	4.47	38.69	13.94	5.50	57.02
7	5.25	42.13	14.20	5.57	61.54
6	5.94	45.35	14.46	5.60	65.73
5	6.57	48.37	14.72	5.61	69.67
4	7.13	51.20	14.98	5.58	73.42
3	7.64	53.76	15.22	5.46	77.03
2	8.04	55.85	15.43	5.03	80.62
1	8.25	56.94	15.54	3.69	84.42

Notes:

1. For flow areas and other data see table 3.
2. 1 lb/min = .00756 kg/s

Table 10. Calculated flow rates (lb/min) in a building with a top vented elevator shaft and a stairwell with a top vent and an open exterior door (Case 5)

Vent and Open Door Flows:		lb/min			
Flow out top vent of elevator shaft		318.71			
Flow out top vent of east stairwell		586.86			
Flow in the open exterior, first floor door of the east stairwell		649.76			

Floor	Into West Stairwell	Into Elevator Shaft	Into East Stairwell	To Floor Above	Into Building From Outside
20	-9.83	-49.61	6.91	-	-57.21
19	-9.55	-47.61	5.89	4.67	-52.68
18	-9.06	-44.03	5.07	6.06	-48.40
17	-8.47	-39.61	4.26	6.43	-43.93
16	-7.83	-34.47	3.35	6.53	-39.02
15	-7.11	-28.31	2.16	6.58	-33.43
14	-6.28	-19.96	-1.15	6.72	-26.85
13	-5.49	-7.79	-3.03	6.16	-17.06
12	-4.30	19.10	-3.85	6.90	10.54
11	-2.33	28.99	-4.39	7.29	23.04
10	2.21	34.91	-5.17	6.51	31.72
9	3.99	40.27	-5.82	6.71	38.32
8	5.22	45.13	-6.41	6.80	43.88
7	6.23	49.57	-6.97	6.84	48.78
6	7.10	53.67	-7.51	6.86	53.22
5	7.88	57.49	-8.05	6.87	57.32
4	8.59	61.06	-8.59	6.85	61.16
3	9.23	64.32	-9.15	6.74	64.84
2	9.75	67.04	-9.78	6.28	68.54
1	10.03	68.53	-10.62	4.73	72.65

Notes:

1. For flow areas and other data see table 3.
2. 1 lb/min = .00756 kg/s

Table 11. Calculated flow rates (lb/min) in a building with a top vented elevator shaft and a stairwell with an open exterior door (Case 6)

Vent and Open Door Flows:						lb/min
Flow out top vent of elevator shaft						342.89
Flow in the open exterior, first floor door of the east stairwell						317.50

Floor	Into West Stairwell	Into Elevator Shaft	Into East Stairwell	To Floor Above	Into Building From Outside
20	-8.22	-37.54	-17.75	-	-67.04
19	-8.03	-36.05	-17.66	3.52	-62.89
18	-7.69	-33.28	-17.51	4.65	-58.79
17	-7.28	-29.82	-17.35	4.95	-54.49
16	-6.85	-25.87	-17.18	4.97	-49.83
15	-6.41	-21.38	-17.02	4.88	-44.64
14	-5.97	-16.16	-16.88	4.70	-38.66
13	-5.57	-9.75	-16.76	4.34	-31.32
12	-5.30	3.81	-16.71	3.54	-20.95
11	-4.30	19.15	-16.45	6.28	-3.96
10	-0.42	32.13	-15.93	8.62	17.16
9	3.55	38.73	-15.58	7.22	26.83
8	5.00	44.15	-15.25	7.08	34.01
7	6.07	48.82	-14.94	6.95	40.04
6	6.96	52.96	-14.65	6.85	45.34
5	7.73	56.72	-14.37	6.77	50.16
4	8.42	60.15	-14.12	6.67	54.62
3	9.02	63.24	-13.89	6.49	58.85
2	9.51	65.75	-13.74	5.99	63.04
1	9.77	67.11	-13.75	4.46	67.58

Notes:

1. For flow areas and other data see table 3.
2. 1 lb/min = .00756 kg/s

Table 12. Calculated flow rates (lb/min) in a building with top vented elevator shaft and stairwell and with elevated shaft and fire floor temperatures (Case 4A)

Vent Flows:		lb/min			
Flow out top vent of elevator shaft		430.68			
Flow out top vent of east stairwell		457.87			

Floor	Into West Stairwell	Into Elevator Shaft	Into East Stairwell	To Floor Above	Into Building From Outside
20	-16.13	-88.65	15.69	-	-81.20
19	-14.89	-80.44	17.15	-7.91	-75.66
18	-13.81	-73.17	18.21	-10.43	-68.19
17	-12.72	-65.68	19.15	-11.03	-59.32
16	-11.51	-57.11	20.08	-10.95	-48.95
15	-10.10	-46.47	21.04	-10.55	-36.18
14	-8.33	-31.33	22.05	-9.92	-16.70
13	-6.31	11.41	22.93	-10.84	31.10
12	-4.79	32.67	23.39	-13.93	51.46
11	-2.65	44.21	23.83	-14.13	66.03
10	2.99	51.73	24.18	-14.78	78.52
9	5.58	59.09	24.59	-14.42	89.00
8	7.44	66.12	25.04	-14.18	98.19
7	9.07	73.17	25.55	-13.78	106.33
6	10.90	81.71	26.24	-12.34	113.05
5	13.51	94.78	27.42	-6.57	117.03
4	10.38	69.99	18.65	12.09	120.15
3	13.83	96.48	27.57	-9.06	131.77
2	13.75	96.08	27.53	-2.98	134.57
1	13.76	96.09	27.54	-0.21	137.14

Notes:

1. For flow areas and other data see table 3.
2. 1 lb/min = .00756 kg/s

Table 13. Calculated flow rates (lb/min) in a building with a top vented elevator shaft, with a stairwell with an open exterior door, and with elevated shaft and fire floor temperatures (Case 6A)

Vent and Open Door Flows:		lb/min			
Flow out top vent of elevator shaft		494.69			
Flow in the open exterior, first floor door of the east stairwell		378.00			

Floor	Into West Stairwell	Into Elevator Shaft	Into East Stairwell	To Floor Above	Into Building From Outside
20	-16.24	-85.77	-10.36	-	-104.63
19	-14.99	-77.17	-11.07	-7.78	-100.44
18	-13.94	-69.68	-12.27	-10.57	-94.89
17	-12.94	-62.36	-13.57	-11.59	-88.42
16	-11.94	-54.67	-14.86	-12.06	-81.14
15	-10.90	-46.21	-16.11	-12.39	-72.88
14	-9.83	-36.55	-17.34	-12.75	-63.25
13	-8.76	-24.75	-18.57	-13.25	-51.29
12	-7.78	-4.30	-19.88	-14.05	-34.10
11	-5.93	37.12	-20.78	-11.91	8.34
10	-1.55	56.47	-21.39	-9.85	35.44
9	5.98	68.02	-22.23	-11.78	51.54
8	8.74	78.18	-23.02	-11.56	63.50
7	10.94	87.65	-23.75	-11.17	73.23
6	13.08	97.73	-24.30	-9.57	80.77
5	15.56	110.06	-24.46	-3.86	85.41
4	11.47	78.57	-14.81	11.88	89.97
3	16.32	113.99	-22.96	-2.88	103.17
2	16.33	114.07	-23.09	1.32	106.45
1	16.37	114.28	-23.22	2.17	109.57

Notes:

1. For flow areas and other data see table 3.
2. 1 lb/min = .00756 kg/s

U.S. DEPT. OF COMM. BIBLIOGRAPHIC DATA SHEET <i>(See instructions)</i>	1. PUBLICATION OR REPORT NO. NISTIR 89-4035	2. Performing Organ. Report No.	3. Publication Date May 1989
4. TITLE AND SUBTITLE Considerations of Stack Effect in Building Fires			
5. AUTHOR(S) John H. Klote			
6. PERFORMING ORGANIZATION <i>(If joint or other than NBS, see instructions)</i> National Institute of Standards and Technology U.S. Department of Commerce Gaithersburg, MD 20899		7. Contract/Grant No.	8. Type of Report & Period Covered
9. SPONSORING ORGANIZATION NAME AND COMPLETE ADDRESS <i>(Street, City, State, ZIP)</i> U.S. Fire Administration Emmitsburg, MD 21727			
10. SUPPLEMENTARY NOTES <input type="checkbox"/> Document describes a computer program; SF-185, FIPS Software Summary, is attached.			
11. ABSTRACT <i>(A 200-word or less factual summary of most significant information. If document includes a significant bibliography or literature survey, mention it here)</i> <p>The following driving forces of smoke movement in buildings are discussed: stack effect, buoyancy of combustion gases, expansion of combustion gases, wind effect, and elevator piston effect. Based on an analysis of elevator piston effect, it is concluded that the likelihood of smoke being pulled into an elevator shaft due to elevator car motion is greater for single car shafts than for multiple car shafts. Methods of evaluating the location of the neutral plane are presented. It is shown that the neutral plane between a vented shaft and the outside is located between the neutral plane height for an unvented shaft [equation (23)] and the vent elevation. Calculations are presented that show that pressure losses due to friction are generally negligible for unvented shafts with all doors closed. The capabilities and limitations of network models and zone models are discussed. The network method was applied to several cases of open and closed doors and shaft vents likely to occur during firefighting. For the cases evaluated, shaft venting did not result in any significant reduction in smoke concentrations on the floors of the building. One of the cases showed that for low outside temperatures, bottom venting of a shaft can result in shaft pressurization. Other cases demonstrated that elevated temperatures of combustion gases can result in downward smoke flow from one floor to another. Much of the information in this paper is applicable to the migration of other airborne matter such as hazardous gases and bacteriological or radioactive matter.</p>			
12. KEY WORDS <i>(Six to twelve entries; alphabetical order; capitalize only proper names; and separate key words by semicolons)</i> elevators; smoke vents; smoke transport; stack effect; stairwells; wind effects			
13. AVAILABILITY <input checked="" type="checkbox"/> Unlimited <input type="checkbox"/> For Official Distribution. Do Not Release to NTIS <input type="checkbox"/> Order From Superintendent of Documents, U.S. Government Printing Office, Washington, D.C. 20402. <input checked="" type="checkbox"/> Order From National Technical Information Service (NTIS), Springfield, VA. 22161		14. NO. OF PRINTED PAGES 92 15. Price \$14.95	

